REVIEW

Magnetocaloric materials for hydrogen liquefaction

Carlos Romero-Muñiz,[1,*] Jia Yan Law,[1] Jorge Revuelta-Losada,[1] Luis M. Moreno-Ramírez,[1] and Victorino Franco[1,*]

*Correspondence: crmuniz@us.es（C.R.-M）; vfranco@us.es (V.F.)

Received: May 16, 2023; Accepted: June 21, 2023; Published Online: December 6, 2023; https://doi.org/10.59717/j.xinn-mater.2023.100045

GRAPHICAL ABSTRACT

PUBLIC SUMMARY

- Magnetic refrigeration is a key enabling technology for hydrogen as an energy vector.
- Adequate material selection is crucial for this application.
- A critical review of over 400 magnetocaloric compounds is provided.

REVIEW

Magnetocaloric materials for hydrogen liquefaction

Carlos Romero-Muñiz,[1,*] Jia Yan Law,[1] Jorge Revuelta-Losada,[1] Luis M. Moreno-Ramírez,[1] and Victorino Franco[1,*]

[1]Departamento de Física de la Materia Condensada, ICMS-CSIC, Universidad de Sevilla, P.O. Box 1065, 41080-Sevilla, Spain

*Correspondence: crmuniz@us.es（C.R.-M）; vfranco@us.es (V.F.)

Received: May 16, 2023; Accepted: June 21, 2023; Published Online: December 6, 2023; https://doi.org/10.59717/j.xinn-mater.2023.100045

Citation: Romero-Muñiz C., Law J.Y., Revuelta-Losada J., et al., (2023). Magnetocaloric materials for hydrogen liquefaction. The Innovation Materials **1(3)**, 100045.

The expected energy transition to hydrogen gas as a greener energy vector has revived the interest in magnetic refrigeration at the cryogenic range, specifically between 20 and 80 K, with the vision to develop a new generation of hydrogen gas liquefiers. From the materials science point of view, the search for magnetocaloric materials containing mainly non-critical elements with a significant response in that temperature range, together with good cyclability and stability, is a challenging task. Given the increasing interest of the research community on this topic, we aim to establish a comprehensive catalog of the magnetocaloric compounds characterized so far, to be used as a starting point for further research. For this purpose, a systematic outlook of the state of the art is presented here, with the analysis and classification of more than 400 cryogenic magnetocaloric materials, divided into five large families according to their physicochemical properties. Moreover, we provide detailed information about their magnetocaloric properties, magnetic behavior, and transition characteristics together with criticality, which will facilitate the future search for optimal compounds.

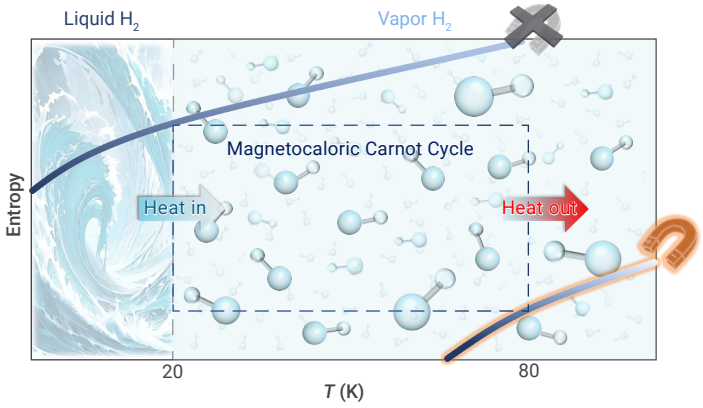

Figure 1. An ideal magnetocaloric Carnot cycle operating between the temperatures of liquid nitrogen (hot reservoir) and liquid hydrogen (cold reservoir) This thermodynamic cycle, and many others, is capable of producing liquid hydrogen starting from liquid nitrogen temperatures.

INTRODUCTION

The current global energy landscape is highly dependent on carbon-based fuels, which have a significant impact on global warming that is already affecting our way of life. This motivates a pressing need to replace our actual energy carriers. For that purpose, the most promising green and clean option is hydrogen gas, and its use is expected to exponentially increase in the years to come.[1-3] Liquefying the gas is a crucial step in the final adoption of hydrogen as an energy vector because of its efficient transportation and storage.[1,2] This will require liquefaction systems to increase energy efficiency, reduce losses, enhance safety, and enable up-scaling; these requirements, up to the moment, are not completely fulfilled by conventional systems based on Joule-Thomson expansion.

To overcome these challenges, refrigeration based on the magnetocaloric effect (MCE) offers the possibility of an alternative and green technology.[3-5] The MCE is defined as the reversible temperature/entropy change produced in a magnetic material subjected to magnetic field variations in adiabatic/isothermal conditions. Since its discovery by P. Weiss and A. Picard in 1917 in nickel at 630 K and its subsequent physical description in 1921 by P. Weiss,[6,7] the capability of the MCE was rapidly exploited. The first breakthrough was in 1933 when W. F. Giauque and D. P. MacDougall[8] reached temperatures below 1 K, using $Gd_2(SO_4)_3{\cdot}8H_2O$, a paramagnetic gadolinium salt, that shows a strong temperature dependence of the magnetization with a large MCE close to zero kelvin. Since those early stages, the possibility of taking advantage of the MCE in every temperature range, depending on the working material, was evidenced, with a larger relevance in the vicinity of magnetic phase transitions where usually the magnetocaloric response is maximized. While paramagnetic salts offer the possibility of achieving ultralow temperatures, it is shown that the use of materials with near-room temperature phase transitions could be used for refrigerators.[9] A paradigmatic example is elemental gadolinium, a ferromagnet with a Curie temperature of 292 K. The research focused on near-room temperature magnetic refrigeration was drastically enhanced at the end of the 20th century by the discovery of materials with an extremely large (or giant) MCE response,[10-15] promoting the fabrication of many working prototypes of refrigerators all over the world.[5] Nowadays, hundreds of magnetocaloric materials have been fully characterized, with transition temperatures ranging from one to several hundred kelvin. These include alloys, intermetallic compounds, oxides, ceramics, molecular solids, etc..[16-20] More recently, an intermediate temperature range between 10 and 80 K is progressively gaining much attention due to its potential applications for gas liquefaction and storage. Given that liquid nitrogen can be produced below 77 K using conventional techniques based on the Hampson-Linde cycle, the challenge arises when trying to obtain other gases of lower boiling points, like hydrogen, in large quantities. Molecular hydrogen has a boiling point of 20.3 K and is one of the very few gases —along with helium and neon —that heats up during thermal expansion, which is a significant drawback for current industrial technology.[21]

Both the cryogenic (below 120 K) and conventional (above 120 K) magnetic refrigeration technologies are considered as energy-efficient alternatives to conventional devices based on mechanical compressors (with an efficiency increase of 50 %[22]).[3-5] The core of these setups is a magnetocaloric material that acts as the working material and is controlled by the application and removal of magnetic field, which is typically generated by permanent or superconducting magnets. In general, the system absorbs heat from a cold load and releases it to the hot reservoir following a standard thermodynamic cycle, such as the ideal Carnot type illustrated in Figure 1, where the intensive variable is magnetic field instead of pressure. The heat transfer between the working material and the reservoirs occurs through a transfer medium made of gas, liquid or the magnetocaloric material itself. The idea of using magnetic refrigeration to produce liquid hydrogen dates to the 1990s, when the first prototypes appeared.[23] Typically, they are designed to use helium as a heat transfer fluid and precooled liquid nitrogen as an input to the hot reservoir. Since compression-based refrigeration has very low efficiencies at cryogenic temperatures (usually less than 20 % of the ideal Carnot efficiency),[24] magnetic refrigeration has been established as a promising alternative to fulfill this industrial requirement. For this purpose, several working prototypes have been built to date.[25-31] The most competitive ones are those based on two-stage active magnetic refrigeration schemes and have already demonstrated good performance.[26,27] Moreover, the use of superconducting magnets is feasible given the operating temperature range of these devices. Thus, devices can operate under high magnetic fields of several tesla. Even so, this technology is still at an early stage of development and if it is to become a fully competitive option for the production of liquid hydrogen, the appropriate selection of magnetocaloric materials must be addressed. The present review article aims to provide a comprehensive reference on magnetocaloric materials suitable for hydrogen liquefaction.

Magnetocaloric working materials can be classified into those undergoing first (FOPT) or second order phase transitions (SOPT). Depending on the application, the magnetic transition should be optimized by modifying its

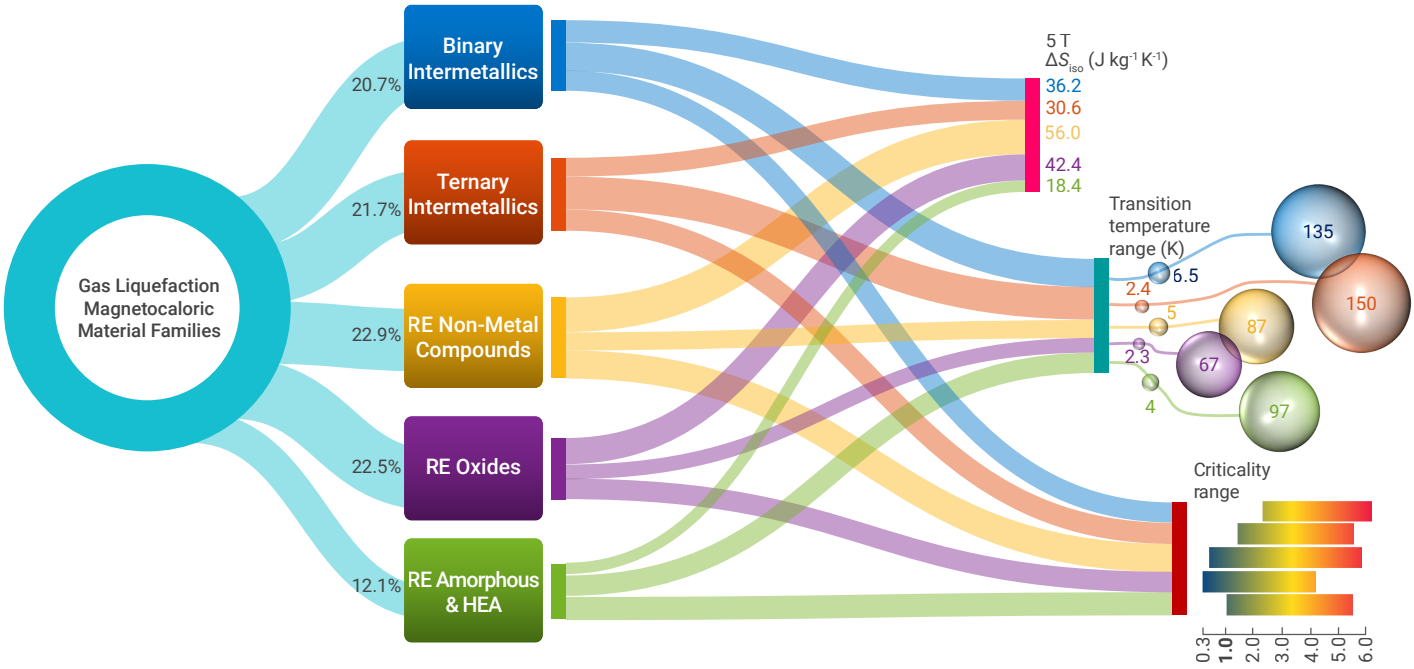

Figure 2. Classification of the cryogenic magnetocaloric materials analyzed in this review For each family of material, with its corresponding importance in the scientific literature, the maximum magnetocaloric response, the temperature range where these materials have a significant response, and the criticality range are shown. The calculation of criticality is explained in the last section of this review.

order or tuning the response towards the desired temperature range. Typically, FOPT responses are larger in magnitude but, at the same time, they usually display thermal hysteresis that hinders the cyclability of the material and seriously affects its performance in devices.[32] For cryogenic applications in the range of 20-80 K, the highest magnetocaloric responses are found in rare-earth (RE) based materials due to their typically low transition temperatures and large magnetic moment.[26,27,29,33] However, the criticality of some elements might prevent its large-scale applications. The reduction of RE elements as well as other critical elements without reducing magnetocaloric response will push forward the industrial implementation of this technology.

This review paper analyzes more than 400 cryogenic magnetocaloric materials suitable for hydrogen liquefaction, paying special attention to composition, magnetocaloric properties, and magnetic phase transition. They are grouped into five different groups or families according to their physicochemical properties, as illustrated in Figure 2. This includes (1) binary and pseudobinary intermetallics; (2) ternary intermetallics with main group elements; (3) borides, nitrides, carbides and chalcogenide compounds (labeled as rare-earth non-metals in the figure); (4) rare-earth oxides; and (5) rare-earth amorphous / high-entropy alloys (HEA). Additionally, open topics pertinent to the material families and their performance are included in this compelling, and critically reviewed, compound materials catalog for gas liquefaction. This is complementary to recent reviews focused on specific families of magnetocaloric materials for cryogenics[34-40] and to a perspective paper on the current trends of magnetocaloric materials.[41]

BRIEF SURVEY ON MAGNETOCALORIC EFFECT CHARACTERIZATION

The MCE is quantified by two complementary magnitudes: the isothermal entropy change (ΔS_{iso}) and the adiabatic temperature change (ΔT_{ad}) driven by a varying magnetic field H. Both ΔS_{iso} and ΔT_{ad} can be measured directly or calculated indirectly through other measured magnitudes, with the indirect calculation of ΔS_{iso} being the most extended in the literature by employing the Maxwell relation:

$$\Delta S_{iso}(T,\Delta H) = \mu_0 \int_0^H \left(\frac{\partial M}{\partial T}\right)_{H'} dH', \quad (1)$$

where μ_0 is the magnetic permeability of vacuum. Similarly, for ΔT_{ad}:

$$\Delta T_{ad}(T,\Delta H) = T\left(exp\left(-\mu_0 \int_0^H \frac{1}{c_H}\left(\frac{\partial M}{\partial T}\right)_{H'} dH'\right) - 1\right), \quad (2)$$

where c is the specific heat. Near the phase transition, if $\Delta T_{ad} \ll T$ and the specific heat (c) is field independent, ΔT_{ad} can be approximated to

$$\Delta T_{ad}(T,\Delta H) \approx -\frac{T\Delta S_{iso}(T,\Delta H)}{c(T)}, \quad (3)$$

although it is based on strong approximations (specially for first-order transitions) and its proper use is not trivial.[42] It has been shown that by employing an effective specific heat in martensitic transformation, it is possible to properly use it for first-order materials.[43] To indirectly obtain ΔT_{ad}, it is much more reliable to calculate it through the total entropy curves obtained from specific heat measurements at different fields:

$$S(T,H) = \int_{0k}^{T} \frac{T'}{c(T',H)} dT', \quad (4)$$

where the entropy at zero kelvin is neglected. Next, ΔT_{ad} is obtained as

$$\Delta T_{ad}(S,\Delta H) = T(S,H) - T(S,0), \quad (5)$$

where $S(T,H)$ is inverted to $T(S,H)$. Similarly, ΔS_{iso} can also be obtained from specific heat measurements as:

$$\Delta S_{iso}(T,\Delta H) = S(T,H) - S(T,0). \quad (6)$$

Other magnitudes derived from ΔS_{iso} and ΔT_{ad} are routinely used to evaluate materials' performance, like the refrigerant capacity (RC), which accounts for the heat that can be exchanged between the hot and cold thermal reservoirs (at temperatures T_{hot} and T_{cold}, respectively).[44] It is calculated as

$$RC = \int_{T_{hot}}^{T_{cold}} |\Delta S_{iso}(T',\Delta H)| dT'. \quad (7)$$

The reservoir temperatures depend on the refrigerator design, but they are usually approximated by the limits of the full width at half maximum

(ΔT_{FWHM}) in the ΔS_{iso} curve. Thus, *RC* can be estimated by the product:

$$RCP = |\Delta S_{iso}^{max}| \cdot \Delta T_{FWHM}, \quad (8)$$

which is known as the relative cooling power (*RCP*). The ΔT_{FWHM} value should be considered with caution because it tends to overestimate the actual temperature span in materials with small magnetocaloric responses. It should be mentioned that more precise magnitudes or parameters have been developed. For instance, the Temperature Averaged Entropy Change (*TEC*),[45] corrects for deceptively large *RC* responses caused by shallow maxima. However, this magnitude is less discussed in the literature and, unfortunately, cannot be used for a general comparison. Similarly, the coefficient of performance (*COP*) offers a more precise tool than *RC* and *RCP* for evaluating the energy conversion of the materials as it also accounts for magnetization hysteresis during working conditions and allows comparison among different cooling technologies.[46] However, this magnitude is also scarcely reported in publications. A recent overview of magnetocaloric measurement techniques, together with their application to the study of phase transitions, is presented in ref.[47]

BINARY INTERMETALLIC COMPOUNDS

Binary compounds between a RE element and a metal, such as transition metal (Fe, Co, Ni, Mn, Cu, Ag, Rh, Pd, etc.), p-block metal (Al, Ga or In) or even a metalloid (Ge or Si) are included in this first group. These compounds can be found in a wide range of stoichiometric combinations, the most prevalent of which are RM, RM_2, R_3M, R_3M_2, RM_5, etc. Even uncommon stoichiometries, such as R_5M_4, R_3M_7 or R_7M_{12}, have a significant impact in this field and their basic magnetic properties have been reported in the last quarter of the previous century.[48] The most relevant compounds with potential applications in cryogenic magnetic refrigeration will be discussed in the following.

Equiatomic compounds with generic formula RM have been extensively studied[40] and some of them display remarkable MCE. The most studied families are RZn, RNi and RGa.

RZn compounds with CsCl-type crystal structure undergo a ferromagnetic to paramagnetic SOPT at 267, 204, 102, 73, 17 and 8.4 K for R = Gd, Tb, Dy, Ho, Er and Tm respectively.[49-52] In addition, a spin reorientation (SR) transition is observed in some of them (R = Tb, Ho and Tm). In particular, HoZn has very broad ΔS_{iso} curves due to two phase transitions, leading to a remarkable refrigerant capacity.[51]

RNi compounds have ferromagnetic behavior with possible low-temperature SR phase transitions at around 10 K. Non-collinear magnetism is observed in all compounds except for GdNi, which is a simple ferromagnet. They crystallize in FeB- or CrB-type crystal structures and their Curie temperatures vary between 8 and 71 K, being GdNi the one with the largest Curie temperature.[53] Thus, the whole series has potential applications for hydrogen liquefaction. Most of them have been characterized for their MCE[54-58] except for the cases of NdNi and TmNi. Overall, from R = Gd to Er they present large values of $|\Delta S_{iso}|$ between 15 and 30 J $kg^{-1}K^{-1}$ for an applied field of 5 T. All of them also exhibit large values of *RC*, especially HoNi. This is due to the coexistence of two phase transitions that leads to a table-like MCE over a broad temperature range. Despite having an intermediate value of ΔS_{iso} of 14.5 J kg^{-1} K^{-1}, the *RCP* value is estimated to be 780 J kg^{-1} for an applied field of 5 T.[56] Zheng et al.[59] have studied the pseudobinary $Ho_xEr_{1-x}Ni$ system for the whole range of x, producing samples with Curie temperatures between 11 and 36 K. The refrigerant capacity increases with increasing Ho content due to the table-like MCE of HoNi.

RGa gallides crystallize with the CrB-type structure and their magnetic properties are rather singular. Except for PrGa and TmGa,[60-62] which display a distinctive behavior including both ferromagnetic and antiferromagnetic ordering, all the rest of the RGa compounds undergo two phase transitions leading to a remarkable MCE.[62-67] One transition is associated with a ferromagnetic ordering, which can be either FOPT or SOPT, and the second is due to a SR transition. The former covers the range of 30-180 K with a decreasing trend from Gd to Er, while the latter always occurs at lower temperatures within the 15-40 K range. They present large values of $|\Delta S_{iso}|$, with TmGa being the one with the largest magnitude. Interestingly, HoGas exhibit two phase transitions occurring at 20 and 69 K, leading to a table-like MCE with a large refrigerant capacity.[62,66] Moreover, the use of solid solutions combining two rare-earth elements is especially suitable for expanding magnetic refrigeration even further in these compounds. For instance, $Tm_{1-x}Ho_xGa$ can be synthesized for all values of x,[62] leading to intermediate compounds exhibiting three phase transitions occurring within a relatively small temperature range. This is because they merge the spin reorientation transition of HoGa with the two successive phase transitions observed in TmGa. Another interesting strategy is to alloy Gd and Er.[68] Since the transition temperatures for GdGa are much higher than those of ErGa, in the $Gd_xEr_{1-x}Ga$ system the ΔS_{iso} peaks can be easily tuned by increasing the content of Gd, achieving compounds with extraordinary refrigerant capacity, as shown in Figure 3A.

Other examples of equiatomic binary compounds mainly crystallize in CsCl structure, such as TmCu, TmAg (both with very poor MCE),[72] $GdCd_{0.8}Ru_{0.2}$,[73] GdRh (both with better MCE responses),[74] NdSi,[75] NdPd,[76] ErAl[77] and HoAl[77] crystallize within orthorhombic DyAl-type structure, where the latter displays successive AFM to FM to PM transitions at 13 and 20 K, leading to remarkable $|\Delta S_{iso}|$ values of 22.5 J kg^{-1} K^{-1} for 5 T.

The MCE of R_2In ferromagnetic compounds reveals a few promising candidates for hydrogen liquefaction. Tb_2In, Dy_2In, Ho_2In and Er_2In crystallize in a Ni_2In-type crystal structure and exhibit Curie temperatures of 165, 130, 82 and 42 K respectively. They possess remarkable MCE [78–81], especially Ho_2In, whose additional SR transition at 32 K on top of the FM to PM transition leads to a large table-like MCE that expands over a broad temperature range.[78] Surprisingly, Eu_2In crystallizes in a different type of crystal structure (Co_2Si-type), exhibits FOPT without apparent hysteresis, and its MCE magnitudes are the largest among the R_2In series, with a maximum $|\Delta S_{iso}|$ of 33 J kg^{-1} K^{-1} at 55 K for an applied field of 5 T (see Figure 3B).[69]

Many RM_2 compounds are known to crystallize within the cubic $MgCu_2$-type crystal structure, or alternatively, the other two so-called Laves phases (i.e., hexagonal $MgZn_2$ or cubic $MgNi_2$). Over the last few years, their magnetic properties have been extensively studied, . Many of them, especially the RNi_2, RCo_2 and RAl_2 series, have been fully characterized for their MCE. RCo_2 compounds could undergo a FOPT with a large MCE associated to it where among them only $HoCo_2$ and $ErCo_2$ show transition temperatures below 80 K (78 and 32 K respectively).[82,83] Both compounds display very large values of $|\Delta S_{iso}|$ and ΔT_{ad}: 20 J kg^{-1} K^{-1} and 8.5 K for $HoCo_2$[84] and 32 J kg^{-1} K^{-1} and 7.2 K for $ErCo_2$[85,86] for an applied field of 5 T. Interestingly, the transition temperature can be finely tuned by alloying two different rare-earth elements[87] or shifted towards lower values after the partial substitution of Co by Ni[84,88] or other elements, as shown in Figure 3C. Solid solutions of RAl_2 compounds have been regarded as potential candidates for low temperature refrigeration since the early days of magnetocaloric research.[89,90] This is because most of these compounds display FM to PM SOPTs between 13 and 80 K with a remarkable MCE.[91] In particular, those compounds with R = Dy, Ho and Er show an additional SR transition below the Curie temperature which enhances their MCE response,[92,93] reaching the outstanding mark of 36.2 J kg^{-1} K^{-1} and 11 K for ΔS_{iso} and ΔT_{ad} respectively for $ErAl_2$.[92] Very recently, Liu et al.[94] have explored the MCE of $NdAl_2$ and $PrAl_2$ together with some of their rare-earth solid solutions leading to remarkable figures. A rather similar behavior but with a lower MCE magnitude has been observed for the RNi_2 series, which has been investigated in depth.[95-100]

For this reason, combinations of RM_2 Laves phases are regarded as strong candidates for hydrogen liquefaction applications and, indeed, are the preferential choice when building operating prototypes.[26,27,29,31] However, it is important to note that, although the RM_2 series with M = Ni, Co and Al has attracted most of the attention in the materials community,[70,101] there are still other combinations that have received less attention despite having promising properties. This is the case with the RMn_2 series[102] or others that have not even been explored yet, like RMg_2. Moreover, it is important to remark that not all RM_2 compounds are Laves phases, like the case of RCu_2 compounds, which adopt an orthorhombic $CeCu_2$-type crystal structure, leading to very interesting magnetic properties.[103-105]

R_3Co might be regarded as another promising family of compounds. They are mainly constituted by rare earth elements, which carry the magnetic moment, while Co acts as nonmagnetic element and, at the same time, stabi-

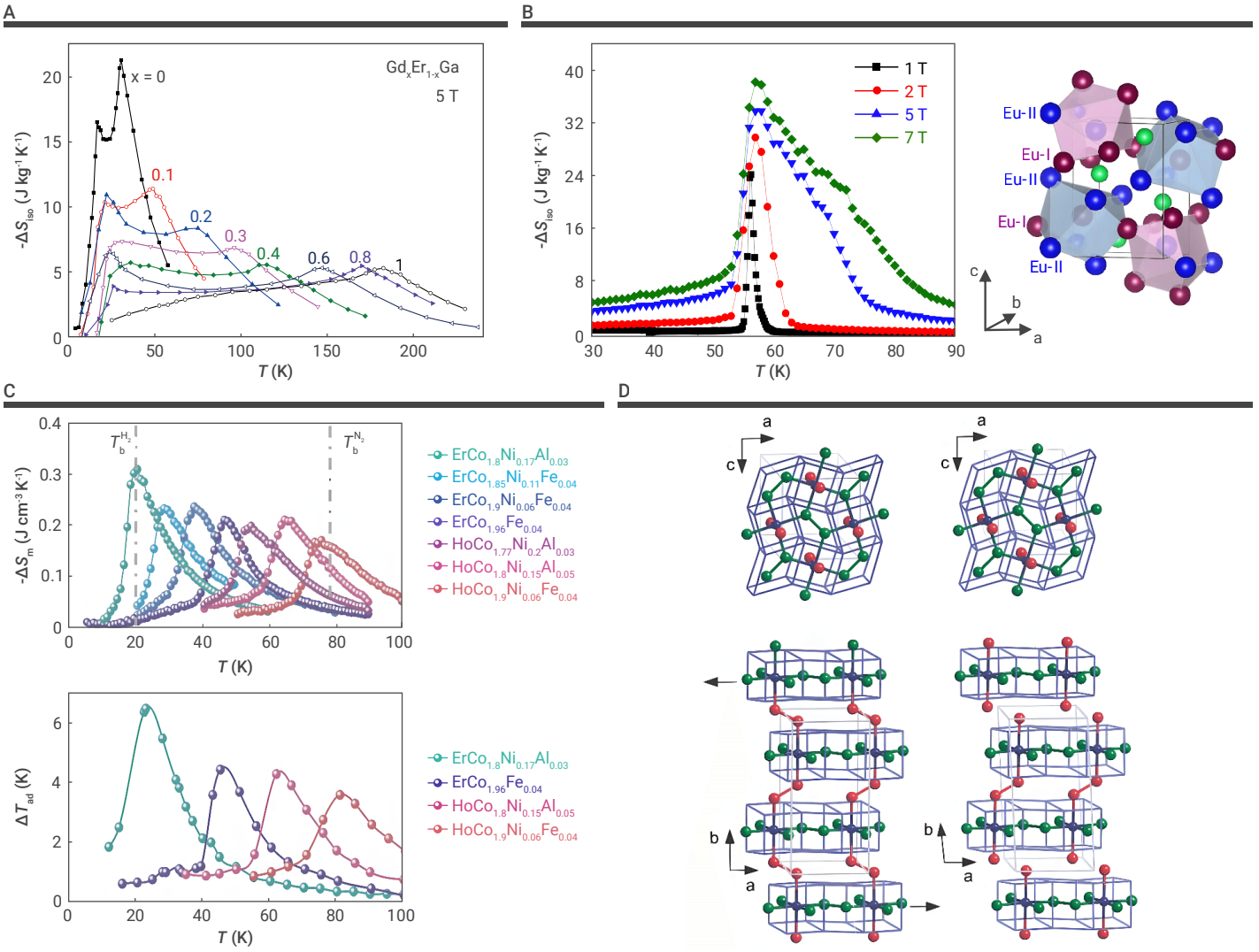

Figure 3. Magnetocaloric response for some promising binary intermetallic materials as well as some examples of representative crystal structures (A) ΔS_{iso} for 5 T for $Gd_xEr_{1-x}Ga$ solid solutions (reproduced with permission of AIP),[68] (B) ΔS_{iso} for 7 T for Eu_2In together with its cell,[69] (C) ΔS_{iso} and ΔT_{ad} for 5 T (upper and lower panel, respectively) for several RM_2 phases[70] and (D) crystal structures of orthorhombic α- (left) and monoclinic β-$Gd_5(Si_2Ge_2)$ (right) (reproduced with permission of APS).[71]

lizes the AF ordering. They crystallize in Fe_3C-type crystal structure and present complex magnetic behavior with transition temperatures between ~5 K (Tm_3Co)[106] and ~130 K (Gd_3Co).[107] Er_3Co, with arguably the best MCE response among the series, shows a very complex non-collinear magnetism and does not follow the general trend observed in the series.[108,109] Most of the other compounds present two close successive phase transitions due to the presence of two types of magnetic orderings. The Tb_3Co,[110] Dy_3Co[111] and Ho_3Co[112] compounds present transition temperatures that fall within the appropriate range between 20 and 80 K, with two peaks or a table-like character observed in their ΔS_{iso} curves, which all give rise to high *RC* values. The transition temperatures of this class of compounds can be easily tuned by either incorporating a new transition metal or rare-earth elements by means of solid solutions. For instance, the Curie temperature of Gd_3Co can be lowered after Ru incorporation in the $Gd_3Co_xRu_{1-x}$.[113,114] Alternatively, the solid solution between Er and Gd allows a great tunability of the transition temperature in $Er_{3-x}Gd_xCo$.[115] There are more compounds with R_3M stoichiometry and most of them have not been systematically studied for magnetocaloric applications. Even so, there are a few promising examples like Gd_3Ru, whose Curie temperature is 54 K and displays a remarkable MCE with $|\Delta S_{iso}|$ values up to 30 J kg^{-1} K^{-1} for 5 T.[116] Again, the solid solution between Gd and Er can be used to adjust the Curie temperature with remarkable precision.[117] Gd_3Rh and Tb_3Rh also show good magnetocaloric properties but with transition temperatures above 100 K.[118,119] In addition, Ho_3Ru and Ho_3Rh have been investigated[120] in samples that contain other secondary phases that also contribute to the global MCE but with moderate performance.

R_3M_2 intermetallic compounds with Er_3Ni_2-type crystal structure are not so common and their MCE performance has not been studied systematically so far. R_3Ni_2 compounds with R = Er and Ho behave as ferromagnets with an additional SR transition at low temperatures.[121] The broad R_3NiCo series, with solid solution of transition metals, have been analyzed by Herrero et al.[122] They present essentially the same features of R_3Ni_2 compounds, same crystal structure and magnetic behavior without a clear SR transition. The Curie temperature monotonically decreases with increasing atomic number through the lanthanide series, from 97 to 7 K, following an almost exact geometric progression with 1/2 of common ratio. *RC* is quite large in these compounds, reaching up to 516 J kg^{-1} for Tb_3NiCo. Similar features are observed in Er_3Rh_2 and Ho_3Rh_2 (despite having a different Y_3Rh_2-type crystal structure), while Nd_3Rh_2 orders antiferromagnetically and shows poorer MCE performance.[123] Another compound with this stoichiometry but with a distinctive tetragonal Zr_3Al_2-type crystal structure is Ho_3Al_2, which displays a spin reorientation transition at 31 K followed by a FM to PM phase transition at 40 K, leading to a remarkable *RC* value of 704 J kg^{-1} for an applied field of 5 T.[124]

The series of RNi_5 is an interesting group of compounds due to its low content in rare-earth elements.[125] They behave as simple ferromagnets with transition temperatures between 10 and 30 K, except $PrNi_5$ which is a param-

agnetic compound with inverse MCE. Among them, $TbNi_5$ and $GdNi_5$ seem more suitable for hydrogen liquefaction, with transition temperatures of 23 K and 32 K respectively[125,126] and remarkable ΔT_{ad}. A very interesting feature of RNi_5 compounds is the possibility to produce ternary compounds of the type RNi_4M or RNi_4X with the incorporation of other metals or nonmagnetic main group elements, which has not yet been systematically studied. For instance, $TbNi_5$ shifts its transition temperature to larger values after partial replacement of Ni by Co or Fe, although its MCE worsens.[126] Conversely, $GdNi_4Al$ and $GdNi_4Si$ display even better MCE than the parent $GdNi_5$ but have slightly lower Curie temperatures.[127]

The $R_5(Si_xGe_{1-x})_4$ pseudobinary alloys have attracted extraordinary attention since the discovery of giant MCE in $Gd_5Si_2Ge_2$ in 1997.[10] From that breakthrough, intense research has focused on this system revealing an extreme complex interplay between their magnetic and crystallographic properties.[71,128-130] In brief, R_5Si_4 and R_5Ge_4 compounds usually crystallize in orthorhombic crystal structures of either Gd_5Si_4- or Sm_5Ge_4-type. However, for intermediate values of x~2, there is a monoclinic phase where the giant MCE could be observed. The FOPT is accompanied by a structural transformation that is responsible for the unexpected large magnetothermal response. The trends in magnetic ordering and transition temperature are difficult to rationalize, but the striking difference in transition temperature between the germanide and silicide counterparts can be attributed primarily to the formation of a different number of covalent bonds between the constituent slabs of the crystal structure in each phase (see Figure 3D). This fact was explained in the case of the Gd based alloy,[71] whose transition temperature gradually drops from 336 K for Gd_5Si_4 to 32 K for Gd_5Ge_4, with all the intermediate values for increasing Ge content. Analogous compounds containing Nd, Tb, Dy and Er have been studied in detail. Nd_5Si_4 and Nd_5Ge_4 display transition temperatures at 71 and 55 K respectively, but with moderate MCE responses.[131] Moreover, it seems that a giant MCE is not observed in the whole $Nd_5(Si_xGe_{1-x})_4$.[131] $Tb_5(Si_xGe_{1-x})_4$ also shows remarkable MCE, but at temperatures above 100 K for the whole x range.[132] $Dy_5(Si_xGe_{1-x})_4$ is a particularly interesting system as its phase transitions expand over a temperature range from 130 K (Dy_5Si_4) to 35 K (Dy_5Ge_4), but its largest MCE is observed for Dy_5Si_3Ge at 65 K, with a ΔS_{iso} larger than 30 J kg^{-1} K^{-1}.[133] In the case of $Er_5(Si_xGe_{1-x})_4$, the phase transitions take place between 14 and 30 K, showing a good yet moderate MCE.[134] Other remarkable compounds include Gd_5Rh_4[74] and especially Gd_5Sn_4,[135] with an excellent MCE response. However, it should be noted that pseudobinary R_5M_4 phases display FOPT, usually with large thermal hysteresis. This means that its use in devices is difficult to implement due to the mechanical degradation of the materials upon operational cyclic conditions and because they usually show poor refrigerant capacities due to the sharp shape of the ΔS_{iso} peaks, despite their large magnitude.

The occupied f-orbitals of lanthanides allow the formation of intermetallic compounds with unusually large stoichiometric coefficients. One example of such type of compounds relevant to magnetocaloric applications is the $R_{12}Co_7$ series. They crystallize following a complicated $Ho_{12}Co_7$-type monoclinic crystal structure containing four different types of coordination polyhedra for the RE sites in the unit cell. The compounds containing Gd, Tb and Dy undergo only one ferromagnetic FM to PM transition at temperatures of 163, 100 and 64 K, respectively.[136-138] Conversely, the compounds with Ho and Er display a more complex behavior, with multiple phase transitions at lower temperatures.[139,140] The possibility of using RE solid solutions to tune the MCE of these compounds had already been demonstrated in $Gd_{12-x}Tb_xCo$[141] and $Er_{12-x}Ho_xCo_7$[140] systems, the latter being very promising for hydrogen liquefaction.

There are a few compounds of the R_5Pd_2 type that have been investigated and they show moderate MCE.[142-144] Related compounds in the form of R_7Pd_3, such as Pr_7Pd_3[145] and Nd_7Pd_3,[146] have also been considered as possible magnetocaloric materials. However, the high content of rare-earth in combination with Pd, an extremely expensive metal, suggests that such compounds are less economical for industrial applications, not even those with remarkable MCE like Nd_7Pd_3.

TERNARY INTERMETALLICS WITH MAIN GROUP ELEMENTS

In this second family of rare-earth compounds, we include those ternary combinations of a lanthanide element, a transition metal and a main group element in addition to Cd or Zn that can be considered in this group.[147] Note that the combinations including non-metal elements of the second period, such as B, C, N or S, will be covered separately in the next section. Similar to binary rare earth compounds, the number of possible combinations in this second family is large. The most common stoichiometries for rare earth ternary compounds are RMX and R_2M_2X. The RMX compounds usually crystallize in a hexagonal ZrNiAl-type crystal structure though other structures could also exist.[148] Their magnetocaloric properties have been investigated in many cases.[37] On the other hand, the magnetocaloric R_2M_2X compounds mainly belong to tetragonal Mo_2FeB_2-type or W_2CoB_2-type crystal structures, along with some other less common structures. Many of these materials are known to display a remarkable MCE.[38] In addition to these most common ones, there are many other stoichiometric possibilities that we will mention throughout this section. For clarity, the discussion thereafter in this section will focus on the various main group elements rather than the different stoichiometry. There are a few relevant cadmium, indium, or magnesium compounds among the ternary rare earth compounds with pertinent magnetocaloric properties, but the majority reported are aluminides, gallides, and silicides.

Aluminides represent a large group of this type of compounds whose magnetocaloric properties have been extensively studied. Magnetic equiatomic compounds, such as ferromagnetic elements (i.e., RNiAl,[149,150] RCoAl[151] and RFeAl[152] series) display good magnetocaloric properties. Those that contain Co and Fe behave as standard ferromagnets whereas those with Ni show antiferromagnetic ordering. The overall MCE performance follows the Co < Ni < Fe trend with transition temperatures in the range 10 - 100 K. Their transition temperatures decrease with increasing atomic mass along the Gd-Er series. Surprisingly, compound series with non-magnetic atoms, such as Cu or Ag, are also promising materials in terms of MCE. If we focus on the RCuAl series, we will find ferromagnetic compounds with Curie temperatures between 81 K for R = Gd to 2.8 K for R = Tm with remarkable $|\Delta S_{iso}|$ values of around 10 - 17 J kg^{-1} K^{-1} and 20 - 30 J kg^{-1} K^{-1} for applied fields of 2 and 5 T, respectively.[153-157] A similar behavior is observed in the RAgAl series but with lower MCE.[158,159]

The remaining interesting aluminides for cryogenic magnetocaloric refrigeration are further combinations of Al with Ni or Co. The series R_2Co_2Al[164,165] and R_2Ni_2Al[165] share some similar features with their equiatomic counterparts, in the sense that Ni compounds display AF behavior while Co compounds behave as ferromagnets. However, their magnetothermal responses are weaker than their RMX counterparts, despite an additional SR transition at low temperatures. Interestingly, $GdNiAl_2$ and $TbNiAl_2$ display remarkable MCE with exceptionally high *RCP* at temperatures around 30 and 20 K respectively,[160] as shown in Figure 4A. Unfortunately, compounds with other lanthanides possess too low transition temperatures. In a similar manner, $R_3Ni_6Al_2$ compounds[166,167] show mainly ferromagnetic behavior and moderate MCE over a broad range of transition temperatures, from 105 K for Gd to 2.5 K for Er. Lastly, R_2CoAl_3 compounds,[168] which are $MgCu_2$-type Laves phases, show SOPTs and lower transition temperatures than their RCo_2 counterparts, with a significantly weaker MCE.

Rare-earth gallides occur in a great variety of combinations and many of them have been fully characterized, showing moderate MCE magnitudes. The MCE of R_2M_2Ga compounds have been reported both for M = Co and Ni.[161,169,170] All of them possess W_2CoB_2-type crystal structure. Co compounds behave as standard ferromagnets and exhibit moderate MCE (see Figure 4B), whereas Ni compounds display AF ordering that transforms to FM in the presence of magnetic fields, resulting in a poor MCE. Other representative compounds include the $RNiGa_2$ series[171] and equiatomic ternary HoAgGa.[172] No MCE characterization of any other compound of the RAgGa series has been reported so far. Compounds with less common stoichiometries, such as R_2CoGa_3[173] or R_6Co_2Ga,[174] have been studied. It is worth noting that despite the moderate magnetothermal response shown by rare-earth gallides, we can find some compounds with a large refrigerant capacity due to the broadness of their ΔS_{iso} curves. This is the case for Gd_6Co_2Ga, whose Curie temperature is 78 K and its *RCP* value is estimated as high as 618 J kg^{-1} for 5 T.[174]

There are many indium compounds containing rare-earth metals showing moderate magnetothermal responses. Although they are characterized by a

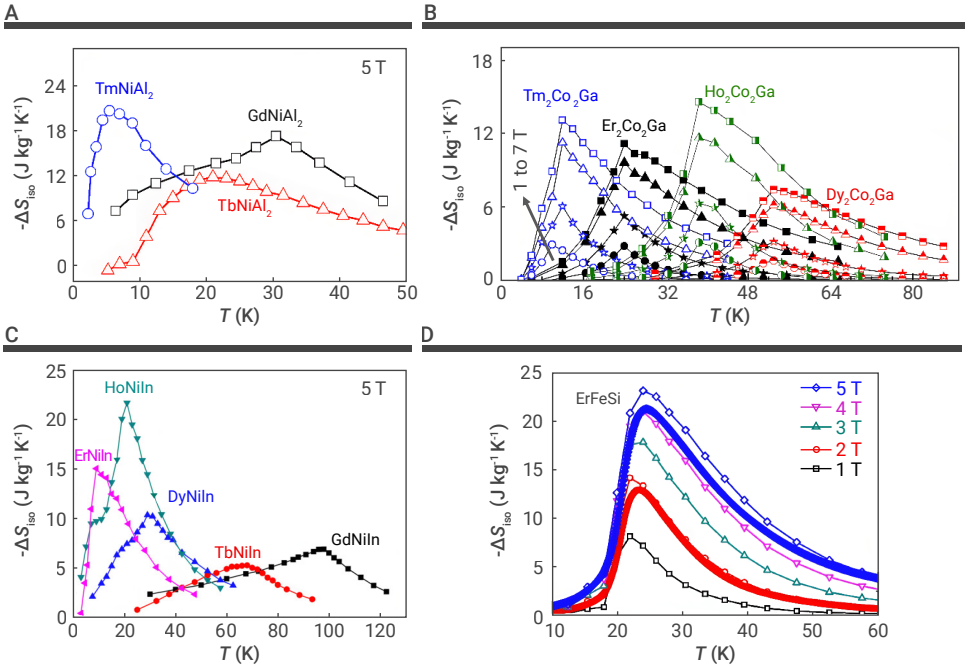

Figure 4. ΔS_{iso} for some promising ternary intermetallic materials (A) $RNiAl_2$ (R=Gd, Tb and Tm) for 5 T,[160] (B) R_2Co_2Ga (R=Dy, Ho, Er and Tm) up to 7 T,[161] (C) RNiIn (R=Gd, Tb, Dy, Ho and Er) for 5 T[162] and (D) ErFeSi for fields up to 5 T from magnetization (symbols) and specific heat (lines) measurements.[163] (All figures reproduced with permission of AIP).

rich variety of magnetic properties and phase transitions, none of them display a relevant MCE. Among them, we highlight the following as representative examples: RNiIn (see Figure 4C),[162] $R_5Ni_2In_4$[175] and R_2Cu_2In[176-178] with ZrNiAl-type, $Lu_5Ni_2In_4$-type and Mo_2FeB_2-type crystal structures, respectively. EuM_5In (M = Cu, Ag and Au) display complex disordered crystal structures and a moderate magnetothermal response.[179] The MCE of the R_2Ni_2In series has also been studied, but their transition temperatures are too low for their use in hydrogen liquefaction.[180]

A few magnesium and cadmium compounds have proven to be excellent candidates for magnetic refrigeration at low temperatures, e.g., equiatomic ternary RPtMg compounds,[181] or the more competitive R_4MMg,[182-184] where M = Pt or Pd. Some of these compounds with Gd_4RhIn-type crystal structure (i.e., Er_4PdMg, Ho_4PtMg or Er_4PtMg) have FM to PM SOPT in the proximity of hydrogen liquefaction temperature with excellent magnetothermal response of $|\Delta S_{iso}|$ around 6 J kg^{-1} K^{-1} and ΔT_{ad} around 2 K for an applied field of 2 T. These values are often used as a good indicator for materials for cryogenic magnetic refrigeration. Isomorphous R_4CoCd compounds also possess excellent MCE, comparable to magnesium compounds.[185,186] In addition, the series R_2Cu_2Cd with Mo_2FeB_2-type crystal structure also shows good MCE properties,[187-189] especially Ho_2Cu_2Cd, whose Curie temperature is 30 K and is accompanied by a SR transition at 15 K, leading to large $|\Delta S_{iso}|$ values around 10 and 20 J kg^{-1} K^{-1} for applied fields of 2 and 5 T, respectively.[189] Unfortunately for these combinations, Pt and Pd are extremely expensive, and Cd is often discouraged due to its high toxicity.

Silicides constitute an extensive family of interesting compounds. For instance, equiatomic ternary compounds, such as HoCoSi,[190] ErFeSi[163] or ErRuSi[191] are well-known ferromagnets with a remarkable MCE and appropriate Curie temperatures (see the ΔS_{iso} curves of ErFeSi in Figure 4D). The main group of silicides are those with the general formula RM_2Si_2 and $ThCr_2Si_2$-type crystal structure, with M = Mn, Cr, Ru, Fe, etc. Most of them present AF behavior with field induced AFM to FM FOPT and a moderate MCE. However, there are some notable exceptions, like $ErCr_2Si_2$,[192] which is a ferromagnet with a SOPT and impressive MCE values: maximum $|\Delta S_{iso}|$ of 24.1 and 29.7 J kg^{-1} K^{-1} and ΔT_{ad} of 8.4 and 17.4 K for 2 and 5 T, respectively. Unfortunately, its Curie temperature is only 4.5 K, which is too low to be considered as a competitive candidate for hydrogen liquefaction applications. Several rare-earth silicides containing Pd have been reported, such as those with the formula RPd_2Si[193,194] or R_2PdSi_3,[195,196] very complex magnetic behavior and poor MCE performance. Note that the Gd_2NiSi_3 compound[197] shares similar features with the aforementioned Pd-containing compounds.

Furthermore, while there are other compositions that contain other main group elements, none of them seem to exhibit a magnetothermal response good enough to be considered for magnetic refrigeration. For example, the study of magnetic properties of R_2Ni_2Sn compounds[198] finds them with extremely complex magnetic behavior and poor MCE magnitude. Other main group element compounds include EuAuZn,[199] EuAgZn,[200] EuPtZn,[200] EuAuGe,[201] $PrMn_{1.4}Fe_{0.6}Ge_2$,[202] or $EuFe_2As_2$.[203]

RARE-EARTH - NON-METAL COMPOUNDS

In this third group of compounds, we discuss rare earth compounds that combine lanthanides with nonmetallic main group elements. This section includes the limiting case of boron element, while those compounds containing oxygen will be discussed exclusively in the next section since oxides constitute a separate and broad group of compounds. Thus, this section focuses mainly on rare earth borides, carbides and nitrides with a few cases of sulfides.

The recent discovery of HoB_2 as a promising candidate for cryogenic magnetic refrigeration[204] has brought renewed attention to boron compounds. This is because HoB_2 possesses one of the largest $|\Delta S_{iso}|$ (about 40 J kg^{-1} K^{-1} for 5 T) near the boiling point of hydrogen, with a ΔT_{ad} of 12 K (see Figure 5A for other values of applied field). This feature was further confirmed by J. Li, et al.,[205] pointing at slightly lower values of about 35 J kg^{-1} K^{-1}. Previously, the magnetocaloric properties of DyB_2 had been studied, with a lower but remarkable MCE.[206] DyB_2 and HoB_2 behave as standard ferromagnets with Curie temperatures at 50 and 15 K respectively, and additional SR transitions at 20 and 12 K. The proximity between the FM to PM and SR phase transitions in HoB_2 might explain the large magnetothermal response observed in this compound. The pseudobinary system formed by the solid solution of Ho and Dy ($Ho_xDy_{1-x}B_2$) has been fully studied for the whole x range.[205,207] The combination of Ho and Dy in the same compound decreases $|\Delta S_{iso}|$ but leads to a table-like response, achieving very large *RC* values of over 600 J kg^{-1}.[205] The Curie temperature can be tuned within the range of 15-50 K depending on the Ho and Dy ratio. More recently, the partial substitution of B by Al has been considered,[208] revealing that the MCE of original HoB_2 is barely affected (including the Curie point) in $HoB_{1.5}Al_{0.5}$. Given the striking price difference between Al and B, this could be a point worth of further exploration. Regarding other members of the RB_2 series, TbB_2 has a too high Curie temperature, i.e., 144 K,[209] while the MCE of ErB_2 or TmB_2 has not yet been investigated.

Other rare-earth borides include the ternary compounds RCo_2B_2 or RCo_3B_2. The RCo_2B_2 series is isomorphous with the RM_2Si_2 silicides that has been discussed in previous section. They crystallize in $ThCr_2Si_2$-type structure and can display either ferromagnetic ordering associated to a SOPT or a metamagnetic FOPT with a field induced AFM to FM transition like $GdCo_2B_2$[217] or $TbCo_2B_2$.[218] As reported by L. Li, et al.[217-220] they display remarkable MCE properties and transition temperatures in the target range for hydrogen liquefaction. Especially, $GdCo_2B_2$ presents large ΔT_{ad} of 6.7 and 15.4 K for 2 T and 5 T, respectively, and also high *RC* in spite of its FOPT. On the other hand, RCo_3B_2 compounds with $CeCo_3B_2$-type crystal structure behave as standard ferromagnets with suitable Curie temperatures for Gd, Tb and Dy compounds. In addition, they display remarkable ΔT_{ad} values even for moderate $|\Delta S_{iso}|$ values.[221-224]

Rare-earth carbides containing transition metals show better overall MCE performance than equivalent borides. Among these carbides, we can highlight the RCoC, $RCoC_2$ and $R_2Cr_2C_3$ series for their excellent MCE. The RCoC

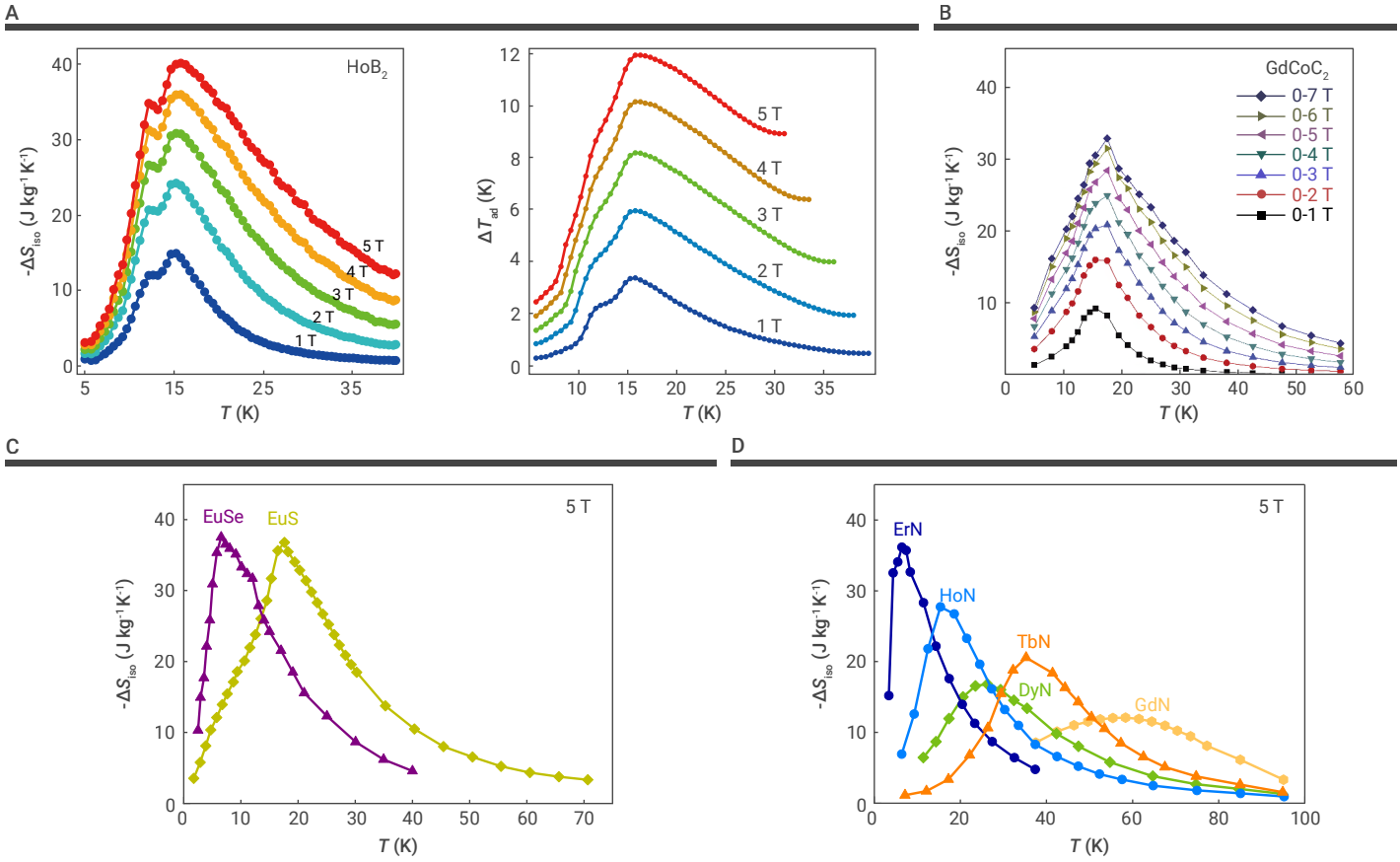

Figure 5. Magnetocaloric response for some promising non-metallic materials (A) Both ΔS_{iso} and ΔT_{ad} (left and right panel, respectively) of HoB_2,[204] (B) ΔS_{iso} of $GdCoC_2$,[210] (C) ΔS_{iso} of EuS and EuSe (data from refs.[211,212]) and (D) ΔS_{iso} of RN (with R=Gd, Tb, Dy, Ho and Er) after data from refs.[213-216]

compounds with R = Tb and Er[225] and $R_2Cr_2C_3$ with R = Dy, Ho and Er[226,227] possess good magnetocaloric properties but their transition temperatures tend to be lower than 25 K. They could undergo either FOPT or SOPT, exhibiting both ferromagnetic and antiferromagnetic ordering depending on the rare earth element, often with a field-induced phase transition from AF to FM order. On the other hand, the whole $RCoC_2$ series with R = Gd, Tb, Ho and Er[210,228,229] behaves as ferromagnetic materials with FM to PM SOPTs. They show low Curie temperatures in the range 11-28 K and large $|\Delta S_{iso}|$. For instance, $GdCoC_2$, whose Curie temperature is 15 K, shows 16 and 28 J kg^{-1} K^{-1} for 2 and 5 T, respectively,[210] as shown in Figure 5B.

Some compounds containing boron and carbon have also been studied for MCE, in particular, the quaternary RNiBC and RM_2B_2C compounds where M = Co and Ni. Those containing cobalt lead to ferromagnetic behavior and SOPTs,[230] while the presence of nickel stabilizes the AFM ordering associated to FOPTs.[231,232] They exhibit characteristics that seem to be more similar to those of carbides than to those of their boride analogs. Equiatomic RNiBC compounds show ferromagnetic ordering and SOPTs, at least for GdNiBC and ErNiBC,[233] but their Curie temperatures are too low even for GdNiBC.

Surprisingly, with the notable exception of EuS, there has been very little research in recent years focused on the magnetocaloric properties of inorganic sulfides. It is a well-known magnetocaloric material[212,234,235] behaving as a ferromagnetic semiconductor with NaCl-type crystal structure and a Curie temperature of 18 K. It displays impressive MCE figures, namely $|\Delta S_{iso}|$ of 22 and 37 J kg^{-1} K^{-1} for 2 and 5 T, respectively, leading to *RCP* values of 284 and 780 J kg^{-1}, respectively. The associated ΔT_{ad} values are 7.5 and 10.4 K, respectively.[212] The analogous EuSe is also a semiconductor that displays excellent MCE. However, its magnetic properties are different: it has a peculiar AF ordering after a FOPT at 4.6 K yet with very broad ΔS_{iso} curves.[211] The ΔS_{iso} curves for 5 T of EuS and EuSe are presented in Figure 5C for comparison.

Typical inorganic sulfides containing rare earth, such as $NaGdS_2$ or $LiGdS_2$, may have an excellent MCE[236] but their transition temperatures are below 10 K. Conversely, there are a few thiospinels with remarkable magnetic properties like $CdCr_2S_4$.[237] This ferromagnetic compound has a Curie temperature of 87 K, slightly above our target temperature range, and show a $|\Delta S_{iso}|$ of 7 J kg^{-1} K^{-1} and a ΔT_{ad} of 2.6 K under an applied field of 5 T. Other related compounds like $FeCr_2S_4$ or $CoCr_2S_4$ possess much higher Curie temperatures.[238] The partial replacement of Cd by Zn in $CdCr_2S_4$ shifts the Curie temperatures to lower values but, at the same time, the MCE magnitude decreases.[239] Notice that spinels are a large family of materials with the general formula of AB_2X_4 that include oxides and other chalcogenide compounds with a unique cubic crystal structure. These compounds allow the accommodation of two different transition metals with both tetrahedral and octahedral coordination. This has led to substantial progress in the development of magnetic materials based on spinel compounds.[240] In summary, further attempts are necessary to find new magnetic sulfides with transition temperatures between 10 and 80 K. We emphasize that even though many sulfides and other chalcogenides do not contain rare-earth elements, their potential as magnetocaloric compounds has not yet been thoroughly studied.

Rare earth nitrides represent another promising group of compounds with distinctive properties and very good MCE features. In particular, rare earth mononitrides with the formula of RN, where R = Gd, Tb, Dy, Ho, Er, have been investigated in depth,[213,214,241] along with many of their binary RE nitrides.[213,215,216,242,243] All of them display NaCl-type crystal structure and a FM to PM SOPT with Curie temperatures in the region of 6 to 60 K, following the usual trend of decreasing Curie temperature along the series Gd < Tb < Dy < Ho < Er (see Figure 5D). They are dense materials in comparison with metallic materials and possess a high thermal conductivity. Rare earth nitrides are very stable from the chemical point of view and do not react with hydrogen gas, in contrast with most intermetallic compounds. For an applied field of 5 T, some of these nitrides, such as HoN or ErN, present very large $|\Delta S_{iso}|$

over 30 J K^{-1} kg^{-1} and ΔT_{ad} around 10 K,[244] whose combined values make them emerge as the magnetocaloric materials with the best performance in the target temperature range (see Figure 5D). More recently, they have been synthesized as nanoparticles which leads to remarkable magnetocaloric properties.[245,246]

RARE-EARTH OXIDES

Magnetic oxides are an extensive class of materials with a great variety of structures and properties. Regarding magnetic ordering, they usually present complex behaviors, including non-collinear magnetism, ferrimagnetism, or multiple phase transitions, often accompanied by structural transformations. Moreover, the presence of more than one magnetic atom in the structure could lead to a distinctive ordering for each species. For instance, there are many oxides that include a rare-earth element and a transition metal (Mn, Cr, Fe, etc.). In these cases, the interplay between 3d and 4f electrons usually plays a major role in the magnetic properties of the compounds, leading to unique features.

From the point of view of the synthesis, oxides follow production methods which clearly differ from those of intermetallic compounds. As a result, the fabrication of relatively large single crystals is usually possible. This feature makes these single crystal potential candidates for rotating magnetocaloric devices in which the refrigeration driving force is created by rotating a strongly anisotropic sample inside a constant magnetic field rather than inducing phase transition on an isotropic material upon changing the modulus of the applied magnetic field. In the case of materials for rotating magnetocaloric applications, the difference between the ΔS_{iso} values obtained along two well-defined crystallographic directions is the key parameter to maximize to obtain an appropriate material, and it is denoted as rotational ΔS_{iso}. The larger the difference between two directions, the larger the refrigerant capacity will be when rotating the sample inside a magnetic field.

For the transition temperatures of oxides, they could range from a few K to more than 1000 K. Most of them undergo phase transitions at very low temperatures, below 10 K, but there are still many examples with higher transition temperatures, such as manganites, ferrites, spinels, etc. In this section, we focus on those with transition temperatures in our target range suitable for hydrogen liquefaction applications. Our discussion proceeds in increasing order of structural complexity, beginning with simple oxides with one metal in the anion (i.e., $RCrO_4$, $RTiO_3$, RVO_4, etc.), and relatively simple structures, such as perovskite and zircon types. Finally, we discuss double oxides that include two metal atoms in the anion site and finalize with garnets and other complex oxides.

Several simple oxides with general stoichiometries of RMO_3 and RMO_4 have been investigated in the framework of magnetocaloric effect. RMO_3 compounds, such as $RCrO_3$, $RFeO_3$, $RTiO_3$, $RMnO_3$ RVO_3, display perovskite-type structure whereas RMO_4 compounds, like $RCrO_4$ or RVO_4, crystallize within the tetragonal zircon-type symmetry. In addition, some spinel oxides could be included in this group. They are the simplest oxides showing a remarkable MCE. To the best of our knowledge, there is no other oxide simpler than these ternary ones with a remarkable MCE, except the notable EuO. This binary oxide crystallizes with a NaCl-type crystal structure and behaves as a ferromagnet with a Curie temperature of 69 K. For an applied field of 5 T, it shows $|\Delta S_{iso}|$ of 17.5 J kg^{-1} K^{-1}, ΔT_{ad} of 6.8 K and *RCP* of 665 J kg^{-1}.[247]

Investigated chromite compounds are of the $RCrO_3$ type, with R = Sm, Dy, Ho, Er, Yb.[248-250] They show antiferromagnetic order and some of them display appropriate transition temperatures like $HoCrO_3$ or $ErCrO_3$, whose transition temperatures are 20 and 10 K, respectively. In general, these compounds show a moderate MCE magnitude, except the aforementioned $ErCrO_3$, with a remarkable value of -13 J kg^{-1} K^{-1} and an associated *RC* of 419 J kg^{-1}.[249]

Single crystals of rare-earth orthoferrites ($RFeO_3$) with orthorhombically distorted perovskite crystal structure have been investigated due to their strong anisotropy along different crystallographic directions.[251-253] The values of rotational isothermal entropy changes between 10 and 20 J kg^{-1} K^{-1} for an applied field of 5 T can be achieved in these materials. Polycrystalline samples of $GdFeO_3$ have also been investigated,[254] where they exhibit very large $|\Delta S_{iso}|$ values, over 30 J kg^{-1} K^{-1} for 5 T, but at around 5 K, which is too low for direct applications in hydrogen liquefaction refrigeration.

Manganites with the general formula of $RMnO_3$ are a well-known class of compounds for the magnetocaloric community since there are hundreds of them fully characterized.[260] Although rare-earth free manganites usually display near-room temperature phase transitions, those with rare-earth elements may have much lower transition temperatures. The investigated $RMnO_3$ includes the magnetocaloric characterization of single crystals where R = Nd,[261] Dy,[262] Tb,[263] Ho[264] and Tm.[265] Another important feature of manganites is that their transition temperatures can be easily tuned by element substitution or pressure. As an example, we can mention the $La_{0.65}Ca_{0.35}Ti_{1-x}Mn_xO_3$ system in which the Curie temperature linearly varies from ~100 K for x=0 to ~40 K for x=0.4.[266] Unfortunately, the MCE magnitude in rare-earth manganites is much weaker than the observed for other related oxides.

Rare-earth titanates ($RTiO_3$) present very interesting magnetocaloric features. They display a relatively simple ferromagnetic ordering compared with other similar oxides and transition temperatures in the range of 30-70 K in most cases. Y Su, et al.[267] systematically studied the MCE of $RTiO_3$ compounds with R = Dy, Ho, Er, Tm, and Yb, revealing very promising properties. The maximumΔS_{iso} values are larger than 10 J kg^{-1} K^{-1} accompanied by remarkable *RCP* values that could be larger than 400 J kg^{-1}. Similar values have been reported for $GdTiO_3$ single crystals.[268] Conversely, a distinctive behavior has been observed for $EuTiO_3$, which orders antiferromagnetically at only 5 K and shows huge $|\Delta S_{iso}|$ and ΔT_{ad} values of 40 J kg^{-1} K^{-1} and 16 K respectively.[269,270]

It is worth noting that the MCE of metavanadates (RVO_3) has not been studied with the exception of $HoVO_3$, whose magnetic properties are clearly distinctive. It undergoes several phase transitions, either due to the Ho^{3+} ion ordering or structural transitions, giving rise to a table-like MCE which spans over a broad temperature range.[271]

On the other hand, some rare-earth chromates ($RCrO_4$) have been studied for R = Gd,[255,272,273] Dy,[274] Ho[255,274] and Er.[272] They crystallize in the tetragonal zircon-type structure and exhibit complex magnetic properties due to the strong competition between ferromagnetic and antiferromagnetic superexchange interactions of 3d and 4f spins. Overall, they behave as ferromagnets but with some anomalies and often with field-induced metamagnetic transitions. Nonetheless, they present remarkable ΔS_{iso} over 20 J kg^{-1} K^{-1} for an applied field of 5 T, as shown in Figure 6A. Notably, other $RCrO_4$ compounds also exhibit transition temperatures between 10 and 25 K and complex magnetic properties, such as non-collinear magnetic ordering.[275,276] Hence, they represent an interesting group of compounds for further investigation of their magnetocaloric properties.

Rare-earth vanadates (RVO_4) are also a particularly interesting family of magnetic oxides. They present excellent magnetocaloric properties but at very low temperatures that are not completely suitable for hydrogen liquefaction purposes.[256,277] This is because their antiferromagnetic order typically occurs below 5 K (see Figure 6B), but their ΔS_{iso} curves are exceptionally broad, leading to a remarkable MCE even at temperatures around 20 K, at least for high fields.[277] A similar behavior is observed for ΔT_{ad}. In spite of this, there are still a few compounds worth highlighting. On the one hand, $HoVO_4$ displays the maximum MCE around 15 K. As it is assumed that its antiferromagnetic ordering occurs at very low temperatures (<1 K), this abnormal feature might be attributed to the crystal-field-split effect of Ho^{3+} ions.[277] On the other hand, compounds such as $TbVO_4$ or $DyVO_4$ show excellent table-like MCE associated to the combination of the AF ordering at 14 K with a subsequent structural transformation from the original tetragonal symmetry to another orthorhombic phase, which takes place at 33 K[257,278] leading to a large conventional and rotating MCE (see Figure 6B). Because of their large relative cooling power and good performance over a broad temperature range, these compounds are particularly interesting.

Double oxides with more complex stoichiometries, such as RM_2O_5, $R_2M_2O_5$, RM_2O_6, $R_2M_2O_6$ (typically with double perovskite structure) or $R_2M_2O_7$, also deserve highlights from the magnetocaloric point of view.

Balli, et al. have studied the rotating MCE of $HoMn_2O_5$[279] and $TbMn_2O_5$[280] due to their strong anisotropy, finding remarkable rotating $|\Delta S_{iso}|$ values over 10 J kg^{-1} K^{-1}. Moreover, $TbMn_2O_5$ exhibits a giant rotating MCE when rotated around the b axis, achieving temperature changes up to 18.7 K.[280] Several cuprates with similar stoichiometries (i.e., $R_2Cu_2O_5$ and R_2BaCuO_5) have been investigated but they usually display inverse MCE and their performance is

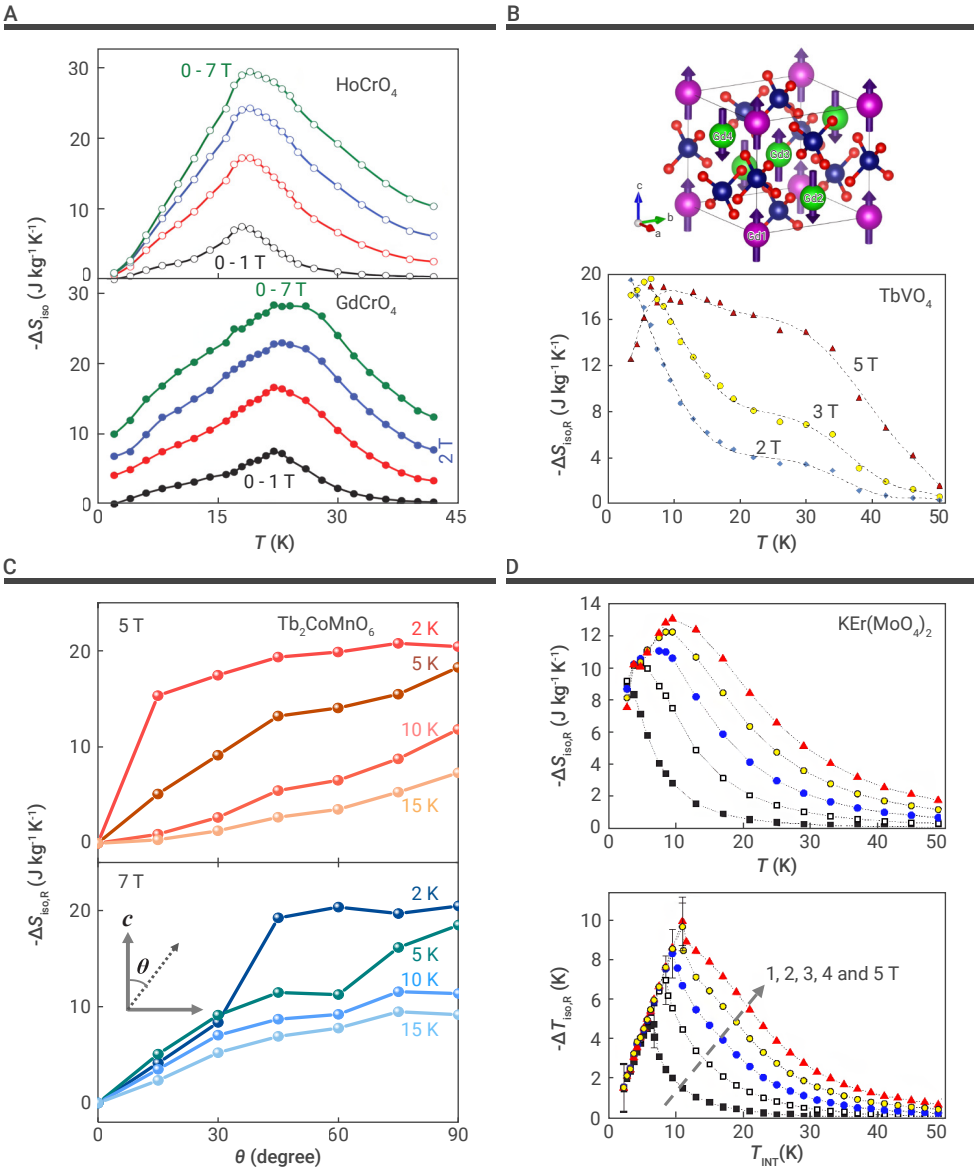

Figure 6. Conventional and rotary magnetocaloric response for some promising oxides (A) Conventional ΔS_{iso} up to 7 T for $RCrO_4$ (R=Gd and Ho),[255] (B) unit cell for RVO_4 oxides with R=Gd (upper panel)[256] and rotational response up to 5 T for R=Tb (lower panel),[257] (C) rotational effect for Tb_2CoMnO_6 for 5 and 7 T (upper and lower panel, respectively)[258] and (D) rotational ΔS_{iso} and ΔT_{ad} (upper and lower panel, respectively) for $KEr(MoO_4)_2$.[259] (All figures are reproduced with permission of AIP and APS.)

limited.[281-283] A larger MCE response is found after substituting Cu by Zn in Dy_2BaZnO_5 or Ho_2BaZnO_5[284] but their transition temperatures shift to very low values.

Polar aeschynite-type oxides with the general formula of $RMWO_6$ attract much attention nowadays due to their exotic magnetic properties and multiferroic character. However, the MCE magnitude in the $RCrWO_6$ series, which has been recently studied, is small,[285-288] often presenting inverse MCE.

Compounds with the general formula of $R_2M_2O_6$ usually crystallize in the so-called double perovskite structure. This structure is obviously closely related to the original perovskite structure of stoichiometry RMO_3 but due to its double nature, it can lead to several substructures that belong to different space groups. The MCE of many RE double perovskites has been investigated[36] but most of them display transition temperatures that are too low for hydrogen liquefaction. However, there are still a few examples with remarkable properties and suitable transition temperatures. The R_2CoMnO_6 series has been studied with more detail for R = Gd, Tb, Dy, Ho and Er.[258,289,290] Despite moderate responses, they present multiple phase transitions, which enables the $|\Delta S_{iso}|$ to span over a broad temperature region between 10 and 100 K,[289] an advantage for refrigeration applications. Gd_2CoMnO_6 possesses the largest MCE among this series, achieving a maximum $|\Delta S_{iso}|$ over 20 J kg^{-1} K^{-1} around 10 K for an applied field of 5 T. An inverse MCE is also observed around 40 K. Interestingly, the partial substitution of Gd by Sr suppresses the inverse MCE without significantly affecting the overall magnetothermal response.[290] The MCE of Tb_2CoMnO_6 single crystals has also been investigated[258] due to their large anisotropy arising from the non-collinear alignment of Mn^{4+}/Co^{2+} spins, which are perpendicular to those of Tb^{3+} ions. Large rotational $|\Delta S_{iso}|$ values between 7.5 and 20 J kg^{-1} K^{-1} can be obtained for an applied field of 5 T at temperatures between 2 and 15 K (see the curves in Figure 6C). It is worth noting that R_2NiMnO_6 double perovskites show similar features, but their transition temperatures are lower than those of their Co counterparts.[291] Other related compounds are R_2FeCrO_6 with R = Er and Tm, which show moderate magnetothermal responses.[292]

Pyrochlores with general stoichiometry of $R_2M_2O_7$ and a distinctive cubic crystal symmetry are an important class of materials with diverse technological applications that might exhibit interesting magnetic behavior.[293] However, their magnetocaloric properties have not been explored in depth and only a few examples can be found in the literature. For instance, Dy_2TiMnO_7, Ho_2TiMnO_7 and $Er_2Mn_2O_7$ behave as standard ferromagnets with SOPTs. The first two compounds display moderate magnetothermal responses with relatively large refrigerant capacities and Curie temperatures around 7.5 K.[294] On the other hand, $Er_2Mn_2O_7$, whose Curie temperature is 34 K, presents very broad ΔS_{iso} curves with a maximum absolute value as large as 16.1 J kg^{-1} K^{-1} for 5 T and a remarkable refrigerant capacity of 522 J kg^{-1},[295] among the largest values of magnetocaloric materials with similar transition temperatures. It is likely that there are other pyrochlores with excellent MCE that have not been investigated.

If we go further in structural complexity, we will find magnetic oxides, such as spinels, complex borates derived or inspired from the mineral gaudefroyite, $KEr(MoO_4)_2$ or a large number of garnets.

Spinel compounds, which have been previously discussed, serve as another feasible magnetocaloric material free of RE elements. X. Luo and coworkers reported on MnV_2O_4,[296] a spinel showing ferrimagnetic ordering below 57 K and a maximum $|\Delta S_{iso}|$ value as large as 24 J kg^{-1} K^{-1} for 4 T. Subsequently, several studies address various partial substitutions in Mn or V sites,[297-299] and reveal the complex nature of the magnetism in this compound. In detail, two successive phase transitions occur near to each other, attributed to the ferrimagnetic ordering and to the t_{2g} orbital ordering of V^{3+} ions at a slightly lower temperature.[298]

Gaudefroyite ($Ca_4Mn_3O_3(BO_3)_3CO_3$) contains chains of edge-linked MnO_6 octahedra on a Kagome lattice, which results in magnetic frustration between the chains and overall spin-liquid behavior below 9 K. Gaudefroyite itself displays a remarkable conventional MCE[300] but, more interestingly, it is possible to synthesize similar compounds, such as $YCa_3Mn_3O_3(BO_3)_4$ or $GdCa_3Mn_3O_3(BO_3)_4$, with better magnetocaloric performance and tunable transition temperature.[300] It is likely that Y could be replaced with other rare-earth. Additionally, related compounds with simplified structures inspired by gaudefroyite have been produced. This is the case for $Pb_{1-x}Sr_xMnBO_4$ with x =

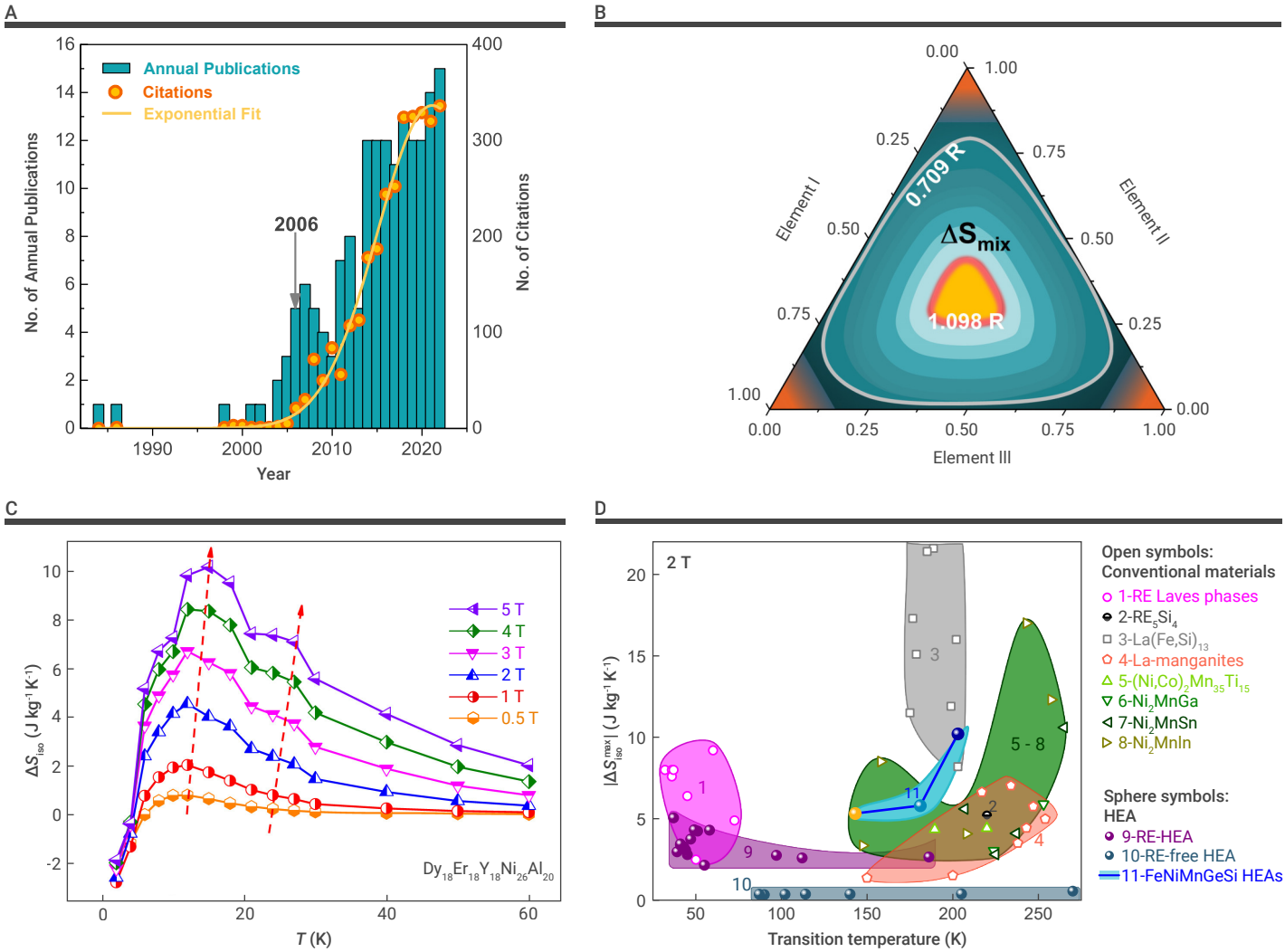

Figure 7. Magnetocaloric amorphous materials (A) Web of Science literature survey on amorphous magnetocaloric annual publications (left y-axis; bar graph) and citations (right y-axis; circles). An exponential increase fits the citation after 2006. Search terms include "amorphous" and "magnetocaloric" in the title field. (B) Contour ΔS_{mix} plot of a model ternary alloy where the conventional alloy compositions are found at the corners. ΔS_{mix} values increase to maximum (at the center of the plot) where the elements are in equimolar concentrations. (C) An example of broad MCE observed in amorphous magnetocaloric HEA. (D) MCE comparison reveals that the amorphous HEA are not competitive to high-performance conventional magnetocaloric materials and the HEA sought by targeted-property search (bluish region). Images B, C, D are reproduced licensed under an open access Creative Commons CC BY license from refs respectively.[310,45,311]

0, 0.5 and 1,[301] which exhibit moderate magnetothermal responses over a broad tunable range of transition temperatures that can be adjusted from 15 to 30 K by varying the Pb/Sr ratio. Other similar borates were reported with better magnetocaloric responses but with much lower transition temperatures.[302] On the other hand, complex oxides like $KEr(MoO_4)_2$ have proven to be excellent candidates for cryogenic magnetic refrigeration[259] due to their large $|\Delta S_{iso}|$ of 14 J kg^{-1} K^{-1} around 10 K for 5 T but, more importantly, the strong magnetic anisotropy in their single crystal. This is because even for moderate fields of 2 T, a remarkable value of 10 J kg^{-1} K^{-1} is obtained with a simple rotation of the single crystal within the ab plane, as shown in Figure 6D.

Lastly, garnets are nesosilicates having the general formula of $X_3Y_2(SiO_4)_3$, being X and Y divalent and trivalent metallic cations. In a more general context, silicon can be replaced by other elements, such as As, V, Fe, Al, etc. Their magnetocaloric properties are well-known from the early days of magnetocaloric research.[303] Due to the large $|\Delta S_{iso}|$ values found at 5 K in gadolinium gallium garnet ($Gd_3Ga_5O_{12}$), also known as GGG, it has been accepted as the standard magnetocaloric material in cryogenic magnetic refrigeration for a very long time.[304] Other rare-earth gallium and aluminum garnets display a similar MCE, showing an overall antiferromagnetic ordering.[303] Unfortunately, the few recent attempts to find garnets with higher transition temperatures lead to poor MCE.[305,306]

RARE-EARTH AMORPHOUS AND HIGH ENTROPY ALLOYS

This last section is devoted to those materials with lack of long-range order and therefore, cannot be considered as crystalline. Very few amorphous alloys had been investigated for MCE, according to early review papers from as early as 2000. Most of the alloys were prepared by rapid solidification with rare-earth elements constituting majority of the alloy composition, typically at least more than 55 atomic %, balanced with transition metal elements. The latter procedure, from a different perspective, dilutes the lanthanide metal, resulting in the broadening of the MCE behavior with very low $|\Delta S_{iso}|$ values though with large temperature spans. In 2006, two related reports, the MCE of Finemet-type alloy[307] and the discovery of universal curves for the field dependence of ΔS_{iso},[308] sparked the transition of rare-earth-based amorphous alloys to transition metal-based compositions, marking a significant turning point for this class of materials. In addition to increased annual publication numbers (see the Web of Science survey presented in Figure 7A), amorphous magnetocaloric alloys show an exponential increase in citations after 2006. Recently, the focus of the work expanded to include amorphous high-entropy alloys (HEA), which use a revolutionary concept for material design, focusing on the central area of multi-principal elements phase diagram (see Figure 7B). Instead of alloying elements to dilute one (or two) base constituent(s) as in case of conventional alloy development (located at the corners of the model ternary phase

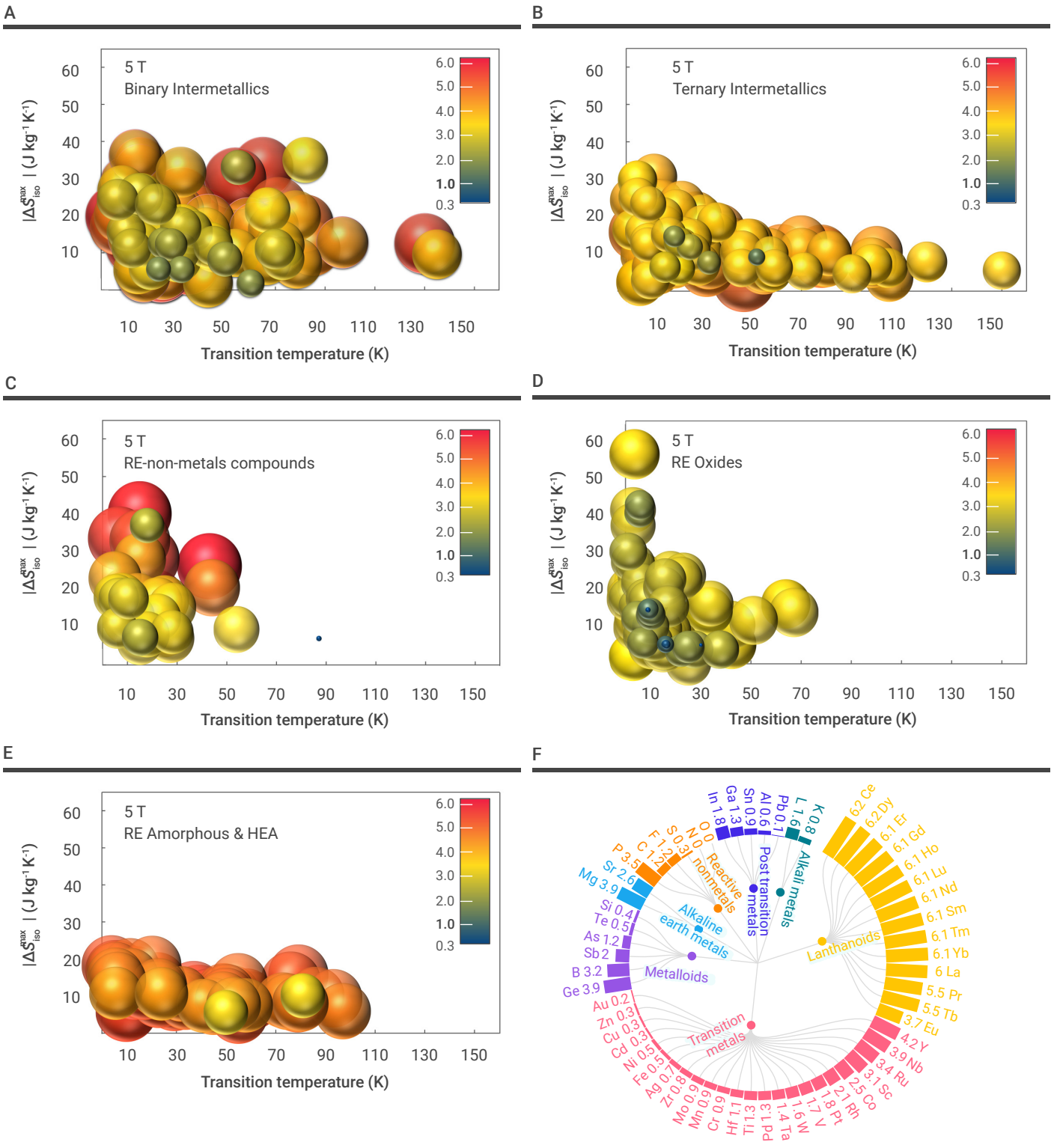

Figure 8. Performance comparison for 5 T considering the weighed criticality supply risk index (A) binary intermetallics, (B) ternary intermetallics, (C) RE non-metals, (D) RE oxides and (E) RE amorphous/HEA. (F) Criticality supply risk of the elements from 2020's EU study.[324]

diagram), the HEA design concept utilizes a blend of several principal elements for a large configuration entropy of mixing (ΔS_{mix}) and thus are dubbed the "high-entropy alloy" name. Their mechanical properties have been found to outperform conventional alloys, thereby underscoring the potential of HEA design to drive the discovery of new materials as well as magnetocaloric materials with optimal mechanical stability.[309]

Initial HEA were restricted to five or more principal elements in equimolar concentrations with the aim of obtaining single-phase metallic solid solutions. In recent years, HEA have evolved to include both intermetallic and ceramic compounds, even with less than five principal elements and in non-equimolar compositions (for further information, readers are recommended to refer to refs.[310,312,313]

Magnetocaloric HEA with amorphous structures are generally designed following the early HEA concept, namely five or more principal elements in equiatomic concentrations, except their atomic radius and enthalpies of mixing (ΔH_{mix}) are largely dissimilar. The reason for this is to form the

desired amorphous structure not just through rapid solidification. Hence, the blend of principal elements involves rare-earth and transition metal elements within the threshold predicted for formation of bulk metallic glass in the HEA space: atomic radius difference $\geq 9\%$, $-35 \leq \Delta H_{mix} \leq -8.5\,kJ\,mol^{-1}$ and $7 \leq \Delta S_{mix} \leq 14\,J\,mol^{-1}K^{-1}$.[314] The common selections are Gd, Dy, Ho, Er, Tm and Tb for RE sites while Fe, Ni, Co, Cu and Al at the transition metal sites. Despite that 60% of the principal elements are RE elements (e.g., three out of five are RE elements in quinary HEA), the RE and transition metal (TM) blend has qualitative properties that are very similar to those of the amorphous conventional alloys mentioned earlier. As a result, amorphous magnetocaloric HEA exhibit broad magnetic ordering transitions and smeared-out MCE behavior (Figure 7C), which are not competitive to conventional magnetocaloric materials with high-performance (see Figure 7D). The same applies to the quaternary RE-TM HEA compositions. In general, they were reported showing spin-glass behavior followed by ferromagnetic-paramagnetic transition and undergo a SOPT. There is a possibility of dilution effects in HEA because the number of elements in the RE and TM sites has increased, but several of them are comparable to those in conventional amorphous RE-based alloys with large ΔS_{iso} values.[315-320] Among the magnetocaloric HEA reports in the cryogenic range, it is worth highlighting as-rolled $FeCoCr_xNi$ HEA, a RE-free composition that could be tuned to lower transition temperatures in the cryogenic range while increasing ΔS_{iso} upon heat treatment when $x \geq 1.05$ (e.g., for $x = 1.15$, transition temperature decreased from ~41 to ~33 K and at the same time with a ~9% increase in ΔS_{iso} upon heat treatment).[321]

Recent targeted property searches in the non-equiatomic HEA space have revealed that magnetocaloric HEA perform competitively or comparably to high-performing conventional magnetocaloric materials.[311,322] Recent review on magnetocaloric HEA reveals that it is possible to search for improved MCE in the non-equiatomic space,[310] even though the current available reports are for temperatures above cryogenic applications. Nonetheless, these results provide insight into applying the HEA design concept for developing magnetocaloric materials with the best possible magnetocaloric and mechanical properties. This also applies to amorphous alloys (low lattice heat capacity) whose transitions are in the cryogenic temperature range.

CONCLUDING REMARKS AND OUTLOOK

In this review, the magnetothermal responses of over 400 cryogenic magnetocaloric materials have been systematically analyzed and categorized, focusing on hydrogen liquefaction applications. This is a crucial step to further guide research on this topic. We have classified the known magnetocaloric materials into different families mainly depending on their chemical composition, finding that each group contains promising materials with some advantages and drawbacks. We have also highlighted families of compounds that are significantly disregarded in the literature, despite their promising potential for magnetocaloric applications.

In addition to this classification, the potential for actual technological applications significantly depends on economic issues. In particular, criticality is a key factor towards the sustainability of any application that aims to be implemented at a large scale. As we have shown, there is extensive literature on the magnetocaloric response of materials, but criticality is usually disregarded in most of the papers. This concept, originally developed for metals, aims to discern among materials that are the most appropriate for a given industrial production process based on the evaluation of three key factors: supply risk, vulnerability to supply restriction, and environmental implications.[323] To put the potential of all the presented materials in the proper context, we have employed the supply risk index (*SRI*) for the different constituents according to the European Commission.[324] This index estimates the risk of disruptions in the supply considering factors such as the supply concentration, import reliance, governance performance measured by the World Governance Indicators, trade restrictions and agreements, existence, and criticality of substitutes. The greater the index, the more critical is the material. The evaluated materials typically range from values close to 0.3 up to 6.1, being considered critical if the index is above 1. For estimating the *SRI* of the alloy, we weighed the index of each constituent by its mass fraction in the composition.

Figure 8 presents, for each of the five major families considered in this review, the transition temperature, the magnetocaloric response (ΔS_{iso}), which determine the location of the data in the figure, together with the *SRI* metrics, represented by the size of the sphere and its color. To make the materials selection easier, compounds with lower *SRI* (less critical) appear more to the front, while the larger *SRI* materials are positioned behind. In this way, less critical materials will be more visible and block the view of less desirable materials for the same ΔS_{iso} and transition temperature ranges. We can see that most of the materials considered are from medium to high criticality, except for the two RE-free spinels. Apart from these cases, the remaining compounds are constituted by lanthanides, often accompanied by critical TM like Pt, Rh, Pd, etc. It is also possible to find other combinations with good MCE performance using less critical metals like Ni, Cu, etc.; however, many of those families exhibit medium criticality. It is therefore not necessary to choose highly critical materials for this specialized application.

Under this scenario, it might seem challenging to find new materials with exceptional magnetic properties that outperform those of the already known compounds, but it is not impossible. In this regard, the comprehensive information provided in this review may constitute a platform to search for new compounds. The recent discovery of the giant MCE in HoB_2[204] by machine learning demonstrates the value of computational screening methods for locating novel compounds with specific target features. The information provided in the supplementary material of this review can be used as a source of input data for such targeted search methodologies or as a reference for more conventional research studies. For example, most of characterization studies are devoted to Gd-Tm compounds while less attention has been paid to Eu compounds despite often showing excellent MCE properties.[69,211,235,247] There are also other families with significant potential to become useful magnetocaloric materials in this temperature range but are currently understudied, like the case for RM_2 Laves phases with M different from M = Co, Ni and Al, spinels, complex oxides or RE borides.

Besides, there is still the challenge of assessing the actual performance of these materials for a particular target application, including the simultaneous use of several materials or composites constituted by multiple phases.[325] The latter has been repeatedly suggested but only a few works performed proper characterization[326,327] for the target temperature range. Moreover, their properties have not been systematically studied for best material combinations.

REFERENCES

1. Al Ghafri, S.Z., Munro, S., Cardella, U., et al. (2022). Hydrogen liquefaction: a review of the fundamental physics, engineering practice and future opportunities. Energy Environ. Sci. ***15***, 2690–2731.
2. Aziz, M. (2021). Liquid hydrogen: A review on liquefaction, storage, transportation, and safety. Energies ***14***, 5917.
3. Sari, O., and Balli, M. (2014). From conventional to magnetic refrigerator technology. Int. J. Refrig. ***37***, 8–15.
4. Franco, V., Blázquez, J., Ipus, J., et al. (2018). Magnetocaloric effect: From materials research to refrigeration devices. Prog. Mater. Sci. ***93***, 112–232.
5. Tušek, J., and Kitanovski, A. (2015). Magnetocaloric energy conversion: From theory to applications. Heidelberg ua: Springer.
6. Weiss, P., and Piccard, A. (1917). Le phénomène magnétocalorique. J. Phys. Theor. Appl. ***7***, 103–109.
7. Weiss, P. (1921). Le phénomène magnéto-calorique. J. Phys. Radium ***2***, 161–182.
8. Giauque, W., and MacDougall, D. (1933). Attainment of temperatures below 1° absolute by demagnetization of $Gd_2(SO_4)_3{\cdot}8H_2O$. Phys. Rev. ***43***, 768.
9. Brown, G. (1976). Magnetic heat pumping near room temperature. J. Appl. Phys. ***47***, 3673–3680.
10. Pecharsky, V.K., and Gschneidner Jr, K.A. (1997). Giant magnetocaloric effect in $Gd_5(Si_2Ge_2)$. Phys. Rev. Lett. ***78***, 4494.
11. Wada, H., and Tanabe, Y. (2001). Giant magnetocaloric effect of $MnAs_{1-x}Sb_x$. Appl. Phys. Lett. ***79***, 3302–3304.
12. Tegus, O., Brück, E., Buschow, K., and De Boer, F. (2002). Transition-metal-based magnetic refrigerants for room-temperature applications. Nature ***415***, 150–152.
13. Liu, J., Gottschall, T., Skokov, K.P., et al. (2012). Giant magnetocaloric effect driven by structural transitions. Nat. Mater. ***11***, 620–626.
14. Fujieda, S., Fujita, A., and Fukamichi, K. (2002). Large magnetocaloric effect in $La(Fe_xSi_{1-x})_{13}$ itinerant-electron metamagnetic compounds. Appl. Phys. Lett. ***81***, 1276–1278.
15. Hu, F.-x., Shen, B.-g., Sun, J.-r., et al. . (2001). Influence of negative lattice expansion and metamagnetic transition on magnetic entropy change in the compound $LaFe_{11.4}Si_{1.6}$. Appl. Phys. Lett. ***78***, 3675–3677.
16. Balli, M., Jandl, S., Fournier, P., and Kedous-Lebouc, A. (2017). Advanced materials

for magnetic cooling: Fundamentals and practical aspects. Appl. Phys. Lett. ***4***, 021305.
17. Kitanovski, A. (2020). Energy applications of magnetocaloric materials. Adv. Energy Mater. ***10***, 1903741.
18. Smith, A., Bahl, C.R., Bjørk, R., et al. (2012). Materials challenges for high performance magnetocaloric refrigeration devices. Adv. Energy Mater. ***2***, 1288–1318.
19. Gschneidner, K.A., Pecharsky, V., and Tsokol, A. (2005). Recent developments in magnetocaloric materials. Rep. Prog. Phys. ***68***, 1479.
20. Evangelisti, M., Luis, F., De Jongh, L., and Affronte, M. (2006). Magnetothermal properties of molecule-based materials. J. Mater. Chem. ***16***, 2534–2549.
21. Al Ghafri, S.Z.S., Munro, S., Cardella, U., et al. (2022). Hydrogen liquefaction: a review of the fundamental physics, engineering practice and future opportunities. Energy Environ. Sci. ***15***, 2690–2731.
22. Zimm, C., Jastrab, A., Sternberg, A., et al. (1998). Description and performance of a near-room temperature magnetic refrigerator. Adv. Cryog. Eng. 1759-1766.
23. Janda, D., DeGregoria, T., Johnson, J., et al. (1991). Design of an active magnetic regenerative hydrogen liquefier. Adv. Cryog. Eng. 891-898.
24. Thirumaleshwar, M., and Subramanyam, S. (1986). Cryogenic refrigeration methods for low and ultra-low temperatures—a review. Sadhana ***9***, 191–232.
25. Iwasaki, W. (2003). Magnetic refrigeration technology for an international clean energy network using hydrogen energy (WE-NET). Int. J. Hydrog. Energy ***28***, 559–567.
26. Kim, Y., Park, I., and Jeong, S. (2013). Experimental investigation of two-stage active magnetic regenerative refrigerator operating between 77 K and 20 K. Cryogenics ***57***, 113–121.
27. Jeong, S. (2014). AMR (Active Magnetic Regenerative) refrigeration for low temperature. Cryogenics ***62***, 193–201.
28. Kamiya, K., Numazawa, T., Matsumoto, K., et al. (2006). Design and build of magnetic refrigerator for hydrogen liquefaction. AIP Conf. Proc. ***823***, 591–597.
29. Numazawa, T., Kamiya, K., Utaki, T., and Matsumoto, K. (2014). Magnetic refrigerator for hydrogen liquefaction. Cryogenics ***62***, 185–192.
30. Matsumoto, K., Kondo, T., Yoshioka, S., et al. (2009). Magnetic refrigerator for hydrogen liquefaction. J. Phys. Conf. Ser. ***150***, 012028.
31. Kamiya, K., Matsumoto, K., Numazawa, T., et al. (2022). Active magnetic regenerative refrigeration using superconducting solenoid for hydrogen liquefaction. Appl. Phys. Express ***15***, 053001.
32. Guillou, F., Yibole, H., Porcari, G., et al. (2014). Magnetocaloric effect, cyclability and coefficient of refrigerant performance in the MnFe (P, Si, B) system. J. Appl. Phys. ***116***, 063903.
33. Zhang, H., Gimaev, R., Kovalev, B., et al. (2019). Review on the materials and devices for magnetic refrigeration in the temperature range of nitrogen and hydrogen liquefaction. Physica B Condens. Matter ***558***, 65–73.
34. Li, L.-W. (2016). Review of magnetic properties and magnetocaloric effect in the intermetallic compounds of rare earth with low boiling point metals. Chin. Phys. B ***25***, 037502.
35. Li, L., and Yan, M. (2020). Recent progresses in exploring the rare earth based intermetallic compounds for cryogenic magnetic refrigeration. J. Alloys Compd. ***823***, 153810.
36. Li, L., and Yan, M. (2023). Recent progress in the development of $RE_2TMTM'O_6$ double perovskite oxides for cryogenic magnetic refrigeration. J. Mater. Sci. Technol. ***136***, 1–12.
37. Zhang, H., and Shen, B.-G. (2015). Magnetocaloric effects in RTX intermetallic compounds (R= Gd–Tm, T= Fe–Cu and Pd, X= Al and Si). Chin. Phys. B ***24***, 127504.
38. Zhang, Y. (2019). Review of the structural, magnetic and magnetocaloric properties in ternary rare earth RE_2T_2X type intermetallic compounds. J. Alloys Compd. ***787***, 1173–1186.
39. H. Zhang, R. Gimaev, B. Kovalev, et al. (2019). Review on the materials and devices for magnetic refrigeration in the temperature range of nitrogen and hydrogen liquefaction. Physica B Condens. Matter. ***558***, 65–73.
40. Zheng, X.-Q., and Shen, B.-G. (2017). The magnetic properties and magnetocaloric effects in binary R–T (R= Pr, Gd, Tb, Dy, Ho, Er, Tm; T= Ga, Ni, Co, Cu) intermetallic compounds. Chin. Phys. B ***26***, 027501.
41. Law, J.Y., Moreno-Ramírez, L.M., Díaz-García, Á., and Franco, V. (2023). Current perspective in magnetocaloric materials research. J. Appl. Phys. ***133***, 040903.
42. Pecharsky, V., and Gschneidner Jr, K. (1999). Magnetocaloric effect from indirect measurements: Magnetization and heat capacity. J. Appl. Phys. ***86***, 565–575.
43. Aznar, A., Gràcia-Condal, A., Planes, A., et al. (2019). Giant barocaloric effect in all-d-metal Heusler shape memory alloys. Phys. Rev. Mater. ***3***, 044406.
44. Wood, M., and Potter, W. (1985). General analysis of magnetic refrigeration and its optimization using a new concept: maximization of refrigerant capacity. Cryogenics ***25***, 667–683.
45. Xue, L., Shao, L., Li, Z., et al. (2022). Utilization of high entropy in rare earth-based magnetocaloric metallic glasses. J. Mater. Res. Technol. ***18***, 5301–5311.
46. Qian, S., Nasuta, D., Rhoads, A., et al. (2016). Not-in-kind cooling technologies: A quantitative comparison of refrigerants and system performance. Int. J. Refrig. ***62***, 177–192.
47. Franco, V. (2021). Magnetocaloric characterization of materials. Magnetic Measurement Techniques for Materials Characterization 697-726.
48. Buschow, K. (1980). Rare earth compounds. Handbook of Ferromagnetic Materials ***1***, 297–414.
49. Wang, X., Wang, L., Ma, Q., et al. (2017). Magnetic phase transitions and large magnetocaloric effects in equiatomic binary DyZn compound. J. Alloys Compd. ***694***, 613–616.
50. Li, L., Yuan, Y., Xu, C., et al. (2017). Observation of large magnetocaloric effect in equiatomic binary compound ErZn. AIP Adv. ***7***, 056401.
51. Li, L., Yuan, Y., Zhang, Y., et al. (2015). Magnetic phase transitions and large magnetic entropy change with a wide temperature span in HoZn. J. Alloys Compd. ***643***, 147–151.
52. Li, L., Yuan, Y., Zhang, Y., et al. (2015). Giant low field magnetocaloric effect and field-induced metamagnetic transition in TmZn. Appl. Phys. Lett. ***107***, 132401.
53. Walline, R., and Wallace, W. (1964). Magnetic and structural characteristics of Lanthanide—Nickel compounds. J. Chem. Phys. ***41***, 1587–1591.
54. Pecharsky, A.O., Mozharivskyj, Y., Dennis, K., et al. (2003). Preparation, crystal structure, heat capacity, magnetism, and the magnetocaloric effect of $Pr_5Ni_{1.9}Si_3$ and PrNi. Phys. Rev. B ***68***, 134452.
55. Drulis, H., Hackemer, A., Zaleski, A., et al. (2011). The magnetocaloric effect and low temperature specific heat of SmNi. Solid State Commun. ***151***, 1240–1243.
56. Kumar, P., Suresh, K., Nigam, A., and Gutfleisch, O. (2008). Large reversible magnetocaloric effect in RNi compounds. J. Phys. D ***41***, 245006.
57. Rajivgandhi, R., Arout Chelvane, J., Quezado, S., et al. (2017). Effect of rapid quenching on the magnetism and magnetocaloric effect of equiatomic rare earth intermetallic compounds RNi (R = Gd, Tb and Ho). J. Magn. Magn. Mater. ***433***, 169–177.
58. Tripathy, S., Suresh, K., Nirmala, R., et al. (2005). Magnetocaloric effect in the intermetallic compound DyNi. Solid State Commun. ***134***, 323–327.
59. Zheng, X., Zhang, B., Wu, H., et al. (2016). Large magnetocaloric effect of $Ho_xEr_{1-x}Ni$ ($0 \le x \le 1$) compounds. J. Appl. Phys. ***120***, 163907.
60. Zheng, X., Chen, J., Xu, Z., et al. (2014). Nearly constant magnetic entropy change and adiabatic temperature change in PrGa compound. J. Appl. Phys. ***115***, 17A938.
61. Mo, Z.-J., Shen, J., Yan, L.-Q., et al. (2013). Low field induced giant magnetocaloric effect in TmGa compound. Appl. Phys. Lett. ***103***, 052409.
62. Yang, S., Zheng, X., Yang, W., et al. (2020). Tunable magnetic properties and magnetocaloric effect of TmGa by Ho substitution. Phys. Rev. B ***102***, 174441.
63. Zheng, X., Xu, J., Shao, S., et al. (2018). Large magnetocaloric effect of NdGa compound due to successive magnetic transitions. AIP Adv. ***8***, 056425.
64. Zheng, X.Q., Chen, J., Shen, J., et al. (2012). Large refrigerant capacity of RGa (R = Tb and Dy) compounds. J. Appl. Phys. ***111***. 07A917.
65. Zhang, J., Luo, J., Li, J., et al. (2009). Magnetic properties and magnetocaloric effect of GdGa compound. J. Alloys Compd. ***469***, 15–19.
66. Chen, J., Shen, B., Dong, Q., and Sun, J. (2010). Giant magnetocaloric effect in HoGa compound over a large temperature span. Solid State Commun. ***150***, 157–159.
67. Chen, J., Shen, B., Dong, Q., et al. (2009). Large reversible magnetocaloric effect caused by two successive magnetic transitions in ErGa compound. Appl. Phys. Lett. ***95***, 132504.
68. Zheng, X., Chen, J., Wang, L., et al. (2014). Magnetic properties and magnetocaloric effects of $Gd_xEr_{1-x}Ga$ ($0 \le x \le 1$) compounds. J. Appl. Phys. ***115***, 17A905.
69. Guillou, F., Pathak, A.K., Paudyal, D., et al. (2018). Non-hysteretic first-order phase transition with large latent heat and giant low-field magnetocaloric effect. Nat. Commun. ***9***, 2925.
70. Tang, X., Sepehri-Amin, H., Terada, N., et al. (2022). Magnetic refrigeration material operating at a full temperature range required for hydrogen liquefaction. Nat. Commun. ***13***, 1817.
71. Choe, W., Pecharsky, V.K., Pecharsky, A.O., et al. (2000). Making and breaking covalent bonds across the magnetic transition in the giant magnetocaloric material $Gd_5(Si_2Ge_2)$. Phys. Rev. Lett. ***84***, 4617.
72. Rawat, R., and Das, I. (2001). The similar dependence of the magnetocaloric effect and magnetoresistance in TmCu and TmAg compounds and its implications. J. Phys. Condens. Matter ***13***, L379.
73. Li, L., Niehaus, O., Johnscher, M., and Pöttgen, R. (2015). Magnetic properties and tuneable magnetocaloric effect with large temperature span in $GdCd_{1-x}Ru_x$ solid solutions. Intermetallics ***60***, 9–12.
74. Wang, C., Zou, J., Liu, J., et al. (2013). Crystal structure, magnetic properties, and the magnetocaloric effect of Gd_5Rh_4 and GdRh. J. Appl. Phys. ***113***, 17A904.
75. Zhang, Q., Gao, R., Cui, L., et al. (2015). Magnetic properties and magnetocaloric effect of the compound NdSi. Physica B Condens. Matter ***456***, 258–260.
76. Wang, Y., Wu, X., Du, Y., et al. (2020). Magnetic properties and magnetocaloric effect of binary compound NdPd. J. Low Temp. Phys. ***198***, 1–10.
77. Yang, L., Zhang, H., Hu, F., et al. (2014). Magnetic and magnetocaloric properties of equiatomic alloys RAl (R= Ho and Er). J. Alloys Compd. ***596***, 58–62.
78. Zhang, Q., Cho, J., Li, B., et al. (2009). Magnetocaloric effect in Ho_2In over a wide temperature range. Appl. Phys. Lett. ***94***, 182501.
79. Zhang, Q., Cho, J., Du, J., et al. (2009). Large reversible magnetocaloric effect in Tb_2In. Solid State Commun. ***149***, 396–399.
80. Zhang, Q., Liu, X., Yang, F., et al. (2009). Large reversible magnetocaloric effect in Dy_2In. J. Phys. D ***42***, 055011.

81. Zhang, H., Shen, B., Xu, Z., et al. (2011). Large reversible magnetocaloric effect in Er_2In compound. J. Alloys Compd. ***509***, 2602–2605.
82. De Oliveira, N., Von Ranke, P., Costa, M.T., and Troper, A. (2002). Magnetocaloric effect in the intermetallic compounds RCo_2 (R= Dy, Ho, Er). Phys. Rev. B ***66***, 094402.
83. Singh, N.K., Suresh, K., Nigam, A., et al. (2007). Itinerant electron metamagnetism and magnetocaloric effect in RCo_2-based Laves phase compounds. J. Magn. Magn. Mater. ***317***, 68–79.
84. Tohei, T., and Wada, H. (2004). Change in the character of magnetocaloric effect with Ni substitution in $Ho(Co_{1-x}Ni_x)_2$. J. Magn. Magn. Mater. ***280***, 101–107.
85. Giguere, A., Foldeaki, M., Schnelle, W., and Gmelin, E. (1999). Metamagnetic transition and magnetocaloric effect in $ErCo_2$. J. Phys. Condens. Matter ***11***, 6969.
86. Wada, H., Tomekawa, S., and Shiga, M. (1999). Magnetocaloric properties of a first-order magnetic transition system $ErCo_2$. Cryogenics ***39***, 915–919.
87. Zhu, Y., Asamoto, K., Nishimura, Y., et al. (2011). Magnetocaloric effect of $(Er_xR_{1-x})Co_2$ (R=Ho, Dy) for magnetic refrigeration between 20 and 80 K. Cryogenics ***51***, 494–498.
88. Wada, H., Tanabe, Y., Shiga, M., et al. (2001). Magnetocaloric effects of Laves phase $Er(Co_{1-x}Ni_x)_2$ compounds. J. Alloys Compd. ***316***, 245–249.
89. Hashimoto, T., Kuzuhara, T., Sahashi, M., et al. (1987). New application of complex magnetic materials to the magnetic refrigerant in an Ericsson magnetic refrigerator. J. Appl. Phys. ***62***, 3873–3878.
90. Gschneidner, K., Takeya, H., Moorman, J., and Pecharsky, V. (1994). $(Dy_{0.5}Er_{0.5})Al_2$: A large magnetocaloric effect material for low - temperature magnetic refrigeration. Appl. Phys. Lett. ***64***, 253-255.
91. Von Ranke, P., De Oliveira, N., Costa, M.T., et al. (2001). The influence of crystalline electric field on the magnetocaloric effect in the series RAl_2 (R= Pr, Nd, Tb, Dy, Ho, Er, and Tm). J. Magn. Magn. Mater. ***226***, 970–972.
92. Von Ranke, P., Pecharsky, V., and Gschneidner, K. (1998). Influence of the crystalline electrical field on the magnetocaloric effect of $DyAl_2$, $ErAl_2$, and $DyNi_2$. Phys. Rev. B ***58***, 12110.
93. Bykov, E., Liu, W., Skokov, K., et al. (2021). Magnetocaloric effect in the Laves-phase $Ho_{1-x}Dy_xAl_2$ family in high magnetic fields. Phys. Rev. Mater. ***5***, 095405.
94. Liu, W., Gottschall, T., Scheibel, F., et al. (2023). Designing magnetocaloric materials for hydrogen liquefaction with light rare-earth Laves phases. J. Phys. Energy ***5***, 034001.
95. Ćwik, J., Koshkid'ko, Y., de Oliveira, N., et al. (2017). Magnetocaloric effect in Laves-phase rare-earth compounds with the second-order magnetic phase transition: Estimation of the high-field properties. Acta Mater. ***133***, 230–239.
96. Ćwik, J., Koshkid'ko, Y., Nenkov, K., et al. (2018). Structural, magnetic and magnetocaloric properties of $HoNi_2$ and $ErNi_2$ compounds ordered at low temperatures. J. Alloys Compd. ***735***, 1088–1095.
97. Ćwik, J., Koshkid'ko, Y., Kolchugina, N., et al. (2019). Thermal and magnetic effects in quasi-binary $Tb_{1-x}Dy_xNi_2$ (x= 0.25, 0.5, 0.75) intermetallics. Acta Mater. ***173***, 27-33.
98. Lai, J., Tang, X., Sepehri-Amin, H., and Hono, K. (2020). Tuning magnetocaloric effect of $Ho_{1-x}Gd_xNi_2$ and $HoNi_{2-y}Coy$ alloys around hydrogen liquefaction temperature. Scripta Mater. ***188***, 302–306.
99. Taskaev, S., Khovaylo, V., Skokov, K., et al. (2020). Magnetocaloric effect in $GdNi_2$ for cryogenic gas liquefaction studied in magnetic fields up to 50 T. J. Appl. Phys. ***127***, 233906.
100. Ćwik, J., Koshkid'ko, Y., Nenkov, K., et al. (2021). Experimental and theoretical analysis of magnetocaloric behavior of $Dy_{1-x}Er_xNi_2$ intermetallics (x= 0.25, 0.5, 0.75) and their composites for low-temperature refrigerators performing an Ericsson cycle. Phys. Rev. B ***103***, 214429.
101. Liu, W., Bykov, E., Taskaev, S., et al. (2022). A study on rare-earth Laves phases for magnetocaloric liquefaction of hydrogen. Appl. Mater. Today ***29***, 101624.
102. Zuo, W., Hu, F., Sun, J., and Shen, B. (2013). Large reversible magnetocaloric effect in RMn_2 (R= Tb, Dy, Ho, Er) compounds. J. Alloys Compd. ***575***, 162–167.
103. Arora, P., Tiwari, P., Sathe, V., and Chattopadhyay, M. (2009). Magnetocaloric effect in $DyCu_2$. J. Magn. Magn. Mater. ***321***, 3278–3284.
104. Karmakar, S., Giri, S., and Majumdar, S. (2015). Observation of large low temperature magnetocaloric effect in $HoCu_2$. J. Appl. Phys. ***117***.
105. Zheng, X., Xu, Z., Zhang, B., et al. (2017). The normal and inverse magnetocaloric effect in RCu_2 (R= Tb, Dy, Ho, Er) compounds. J. Magn. Magn. Mater. ***421***, 448–452.
106. Mo, Z.-J., Shen, J., Yan, L.-Q., et al. (2013). Low-field induced large reversible magnetocaloric effect in Tm_3Co compound. J. Alloys Compd. ***572***, 1–4.
107. Tripathy, S., Suresh, K., and Nigam, A. (2006). A comparative study of the magnetocaloric effect in Gd_3Co and Gd_3Ni. J. Magn. Magn. Mater. ***306***, 24–29.
108. Kumar, P., Singh, N.K., Nayak, A.K., et al. (2010). Large reversible magnetocaloric effect in Er_3Co compound. J. Appl. Phys. ***107***, 09A932.
109. Jun, S., Jin-Liang, Z., Feng-Xia, H., et al. (2010). Order of magnetic transition and large magnetocaloric effect in Er_3Co. Chin. Phys. B ***19***, 047502.
110. Li, B., Du, J., Ren, W., et al. (2008). Large reversible magnetocaloric effect in Tb_3Co compound. Appl. Phys. Lett. ***92***, 242504.
111. Shen, J., Zhao, J.-L., Hu, F.-X., et al. (2010). Magnetocaloric effect in antiferromagnetic Dy_3Co compound. Appl. Phys. A ***99***, 853–858.
112. Shen, J., and Wu, J.-F. (2011). Magnetocaloric effect and magnetic phase transition in Ho_3Co. J. Appl. Phys. ***109***, 07A931.
113. Shang, Y., Cao, Y., Balfour, E.A., et al. (2018). The effect of Co substitution on the magnetic and magnetocaloric properties of Gd_3Ru. J. Magn. Magn. Mater. ***451***, 368–372.
114. Monteiro, J., dos Reis, R., and Gandra, F. (2018). Role of electronic and structural characteristics on the magnetic properties of the $Gd_3Co_{1-x}Ru_x$ series. J. Alloys Compd. ***768***, 1–5.
115. Mo, Z.-J., Shen, J., Yan, L.-Q., et al. (2013). Magnetic properties and magnetocaloric effects in $Er_{3-x}Gd_xCo$ intermetallic compounds. J. Appl. Phys. ***113***, 033908.
116. Monteiro, J.C.B., Dos Reis, R., and Gandra, F. (2015). The physical properties of Gd_3Ru: A real candidate for a practical cryogenic refrigerator. Appl. Phys. Lett. ***106***, 194106.
117. Monteiro, J., and Gandra, F. (2019). Magnetocaloric properties of $(Gd_{1-x}Er_x)_3Ru$ alloys and their composites. J. Alloys Compd. ***803***, 1178–1183.
118. Talik, E., and Klimczak, M. (2009). Giant magnetocaloric effect in Tb_3Rh. J. Alloys Compd. ***486***, L30–L33.
119. Kumar, P., Suresh, K., and Nigam, A. (2011). Magnetothermal effect in Gd_3Rh. J. Appl. Phys. ***109***, 07A909.
120. Shang, Y., Yuan, Y., Cao, Y., et al. (2020). Structure, magnetic properties, and magnetocaloric effect of polycrystalline Ho_3M (M= Rh, Ru) alloys. J. Magn. Magn. Mater. ***497***, 166055.
121. Dong, Q., Chen, J., Shen, J., et al. (2011). Magnetic properties and magnetocaloric effects in R_3Ni_2 (R= Ho and Er) compounds. Appl. Phys. Lett. ***99***, 132504.
122. Herrero, A., Oleaga, A., Provino, A., et al. (2021). Crystallographic, magnetic and magnetocaloric properties in novel intermetallic materials R_3CoNi (R= Tb, Dy, Ho, Er, Tm, Lu). J. Alloys Compd. ***865***, 158948.
123. Wang, Y., Du, Y., Zhang, Y., et al. (2020). Low-temperature magnetic properties and large magnetocaloric effects in the RE_3Rh_2 (RE= Nd, Ho and Er) intermetallics. Intermetallics ***127***, 106989.
124. Zhang, H., Xu, Z., Zheng, X., et al. (2012). Giant magnetic refrigerant capacity in Ho_3Al_2 compound. Solid State Commun. ***152***, 1127–1130.
125. Von Ranke, P., Mota, M., Grangeia, D., et al. (2004). Magnetocaloric effect in the RNi_5 (R= Pr, Nd, Gd, Tb, Dy, Ho, Er) series. Phys. Rev. B ***70***, 134428.
126. Haldar, A., Dhiman, I., Das, A., et al. (2011). Magnetic, magnetocaloric and neutron diffraction studies on $TbNi_{5-x}M_x$ (M= Co and Fe) compounds. J. Alloys Compd. ***509***, 3760–3765.
127. Toliński, T., Falkowski, M., Synoradzki, K., et al. (2012). Magnetocaloric effect in the ferromagnetic $GdNi_4M$ (M= Al, Si) and antiferromagnetic $NdNiAl_4$ compounds. J. Alloys Compd. ***523***, 43–48.
128. Pecharsky, V.K., and Gschneidner Jr, K.A. (1997). Tunable magnetic regenerator alloys with a giant magnetocaloric effect for magnetic refrigeration from ~20 to ~290 K. Appl. Phys. Lett. ***70***, 3299–3301.
129. Pecharsky, V.K., and Gschneidner Jr, K.A. (2001). $Gd_5(Si_xGe_{1-x})_4$: An extremum material. Adv. Mater. ***13***, 683–686.
130. Pecharsky, V.K., Samolyuk, G.D., Antropov, V.P., et al. (2003). The effect of varying the crystal structure on the magnetism, electronic structure and thermodynamics in the $Gd_5(Si_xGe_{1-x})_4$ system near x=0.5. J. Solid State Chem. ***171***, 57-68.
131. Gschneidner Jr, K., Pecharsky, V., Pecharsky, A., et al. (2000). The nonpareil $R_5(Si_xGe_{1-x})_4$ phases. J. Alloys Compd. ***303***, 214–222.
132. Morellon, L., Magen, C., Algarabel, P.A., et al. (2001). Magnetocaloric effect in $Tb_5(Si_xGe_{1-x})_4$. Appl. Phys. Lett. ***79***, 1318–1320.
133. Ivtchenko, V., Pecharsky, V., and Gschneidner, K. (2000). Magnetothermal Properties of $Dy_5(Si_xGe_{1-x})_4$ Alloys. Adv. Cryog. Eng. Mater. ***46***, 405–412.
134. Pecharsky, A., Gschneidner Jr, K.A., Pecharsky, V.K., et al. (2004). Phase relationships and structural, magnetic, and thermodynamic properties of alloys in the pseudobinary Er_5Si_4–Er_5Ge_4 system. Phys. Rev. B ***70***, 144419.
135. Ryan, D., Elouneg-Jamróz, M., Van Lierop, J., et al. (2003). Field and temperature induced magnetic transition in Gd_5Sn_4: a giant magnetocaloric material. Phys. Rev. Lett. ***90***, 117202.
136. Chen, X., and Zhuang, Y. (2008). Magnetocaloric effect of $Gd_{12}Co_7$. Solid State Commun. ***148***, 322–325.
137. Deng, J., Zhuang, Y., Li, J., and Huang, J. (2007). Magnetic properties of $Tb_{12}Co_7$. Physica B Condens. Matter ***391***, 331–334.
138. Dong, Q., Chen, J., Zhang, X., et al. (2013). Magnetic phase transition and magnetocaloric effect in $Dy_{12}Co_7$ compound. J. Appl. Phys. ***114***, 173911.
139. Zheng, X., Shao, X., Chen, J., et al. (2013). Giant magnetocaloric effect in $Ho_{12}Co_7$ compound. Appl. Phys. Lett. ***102***, 022421.
140. Zheng, X., Zhang, B., Li, Y., et al. (2016). Large magnetocaloric effect in $Er_{12}Co_7$ compound and the enhancement of δT_{FWHM} by Ho-substitution. J. Alloys Compd. ***680***, 617–622.
141. Zheng, Z., Zhong, X., Yu, H., et al. (2011). Magnetic phase transitions and magnetocaloric properties of $(Gd_{12-x}Tb_x)Co_7$ alloys. J. Appl. Phys. ***109***, 07A919.
142. Samanta, T., Das, I., and Banerjee, S. (2007). Magnetocaloric effect in Ho_5Pd_2: Evidence of large cooling power. Appl. Phys. Lett. ***91***, 082511.
143. Sharma, M.K., and Mukherjee, K. (2018). Evidence of large magnetic cooling power and double glass transition in Tb_5Pd_2. J. Magn. Magn. Mater. ***466***, 317–322.
144. Sharma, M.K., Kaur, G., and Mukherjee, K. (2019). Nature of glassy magnetic state in magnetocaloric materials $Dy_5Pd_{2-x}Ni_x$ (x= 0 and 1) and universal scaling analysis of R_5Pd_2 (R= Tb, Dy and Er). J. Alloys Compd. ***782***, 10–16.
145. Du, Y., Li, C., Cheng, G., et al. (2018). Investigation on the Magnetocaloric Effect of

the Pr_7Pd_3 Compound. J. Supercond. Nov. Magn. ***31***, 2573–2577.

146. Singh, N.K., Kumar, P., Mao, Z., et al. (2009). Magnetic, magnetocaloric and magnetoresistance properties of Nd_7Pd_3. J. Phys. Condens. Matter ***21***, 456004.
147. Jensen, W.B. (2003). The place of zinc, cadmium, and mercury in the periodic table. J. Chem. Educ. ***80***, 952–961.
148. Gupta, S., and Suresh, K. (2015). Review on magnetic and related properties of RTX compounds. J. Alloys Compd. ***618***, 562–606.
149. Oboz, M., and Talik, E. (2011). Properties of the GdTX (T= Mn, Fe, Ni, Pd, X= Al, In) and $GdFe_6Al_6$ intermetallics. J. Alloys Compd. ***509***, 5441–5446.
150. Singh, N.K., Suresh, K., Nirmala, R., et al. (2007). Effect of magnetic polarons on the magnetic, magnetocaloric, and magnetoresistance properties of the intermetallic compound HoNiAl. J. Appl. Phys. ***101***, 093904.
151. Zhang, X., Wang, F., and Wen, G. (2001). Magnetic entropy change in RCoAl (R= Gd, Tb, Dy, and Ho) compounds: candidate materials for providing magnetic refrigeration in the temperature range 10 K to 100 K. J. Phys. Condens. Matter ***13***, L747.
152. Zhang, Y., Wilde, G., Li, X., et al. (2015). Magnetism and magnetocaloric effect in the ternary equiatomic REFeAl (RE= Er and Ho) compounds. Intermetallics ***65***, 61–65.
153. Dong, Q., Shen, B., Chen, J., et al. (2009). Large reversible magnetocaloric effect in DyCuAl compound. J. Appl. Phys. ***105***, 113902.
154. Dong, Q., Shen, B., Chen, J., et al. (2009). Magnetic properties and magnetocaloric effects in amorphous and crystalline GdCuAl ribbons. Solid State Commun. ***149***, 417–420.
155. Dong, Q., Chen, J., Shen, J., et al. (2012). Large magnetic entropy change and refrigerant capacity in rare-earth intermetallic RCuAl (R= Ho and Er) compounds. J. Magn. Magn. Mater. ***324***, 2676–2678.
156. Wang, L., Dong, Q., Mo, Z., et al. (2013). Low-temperature reversible giant magnetocaloric effect in the HoCuAl compound. J. Appl. Phys. ***114***, 163915.
157. Mo, Z.-J., Shen, J., Yan, L.-Q., et al. (2013). Low-field induced giant magnetocaloric effect in TmCuAl compound. Appl. Phys. Lett. ***102***, 192407.
158. Singh, N.K., Kumar, P., Suresh, K., and Nigam, A. (2009). Investigations on magnetic and magnetocaloric properties of the intermetallic compound TbAgAl. J. Appl. Phys. ***105***, 023901.
159. Zhang, Y., Yang, B., and Wilde, G. (2015). Magnetic properties and magnetocaloric effect in ternary REAgAl (RE= Er and Ho) intermetallic compounds. J. Alloys Compd. ***619***, 12–15.
160. Xu, J., Zheng, X., Yang, S., et al. (2019). Low working temperature near liquid helium boiling point of $RNiAl_2$ (R= Tm, Tb and Gd) compounds with large magnetocaloric effect. J. Appl. Phys. ***125***, 225102.
161. Zhang, Y., Guo, D., Geng, S., et al. (2018). Structure, magnetic and cryogenic magneto-caloric properties in intermetallic gallium compounds RE_2Co_2Ga (RE= Dy, Ho, Er, and Tm). J. Appl. Phys. ***124***, 043903.
162. Zhang, H., Xu, Z., Zheng, X., et al. (2011). Magnetocaloric effects in RNiIn (R= Gd-Er) intermetallic compounds. J. Appl. Phys. ***109***, 123926.
163. Zhang, H., Shen, B., Xu, Z., et al. (2013). Large reversible magnetocaloric effects in ErFeSi compound under low magnetic field change around liquid hydrogen temperature. Appl. Phys. Lett. ***102***, 092401.
164. Morozkin, A., Genchel, V., Garshev, A., et al. (2017). Magnetic ordering of Mo_2NiB_2-type {Gd, Tb, Dy)$_2Co_2Al$ compounds by magnetization and neutron diffraction study. J. Magn. Magn. Mater. ***442***, 36–44.
165. Dong, X., Feng, J., Yi, Y., and Li, L. (2018). Investigation of the crystal structure and cryogenic magnetic properties of RE_2T_2Al (RE= Dy, Ho, Er, and Tm; T= Co and Ni) compounds. J. Appl. Phys. ***124***, 093901.
166. Li, D., Nimori, S., and Aoki, D. (2013). Magnetic entropy change and relative cooling power of $Gd_3Ni_6Al_2$ and $Tb_3Ni_6Al_2$ compounds. Solid State Commun. ***156***, 54–58.
167. Xu, J., Zheng, X., Yang, S., et al. (2021). Large reversible magnetic entropy change of $R_3Ni_6Al_2$ (R= Dy, Ho and Er) compounds. J. Alloys Compd. ***879***, 160468.
168. Meng, L., Jia, Y., Qi, Y., et al. (2017). Investigation of the magnetism and magnetocaloric effect in the R_2CoAl_3 (R= Gd, Tb, Dy, and Ho) compounds. J. Alloys Compd. ***715***, 242–246.
169. Zhang, Y., Yang, Y., Hou, C., et al. (2018). Metamagnetic transition and magnetocaloric properties in antiferromagnetic Ho_2Ni_2Ga and Tm_2Ni_2Ga compounds. Intermetallics ***94***, 17–21.
170. Guo, D., Li, H., and Zhang, Y. (2018). Magnetic phase transition and magnetocaloric effect in ternary Er_2Ni_2Ga compound. IEEE T. Magn. ***55***, 1–4.
171. Guo, D., Moreno-Ramírez, L.M., Law, J.-Y., et al. (2023). Excellent cryogenic magnetocaloric properties in heavy rare-earth based $HRENiGa_2$ (HRE= Dy, Ho, or Er) compounds. Sci. China Mater. ***66***, 249–256.
172. Da Silva, L., Dos Santos, A., Coelho, A., and Cardoso, L. (2013). Magnetic properties and magnetocaloric effect of the HoAgGa compound. Appl. Phys. Lett. ***103***, 162413.
173. Wang, L., Cui, L., Dong, Q., et al. (2014). Large magnetocaloric effect with a wide working temperature span in the R_2CoGa_3 (R= Gd, Dy, and Ho) compounds. J. Appl. Phys. ***115***, 233913.
174. Guo, D., Moreno-Ramírez, L.M., Romero-Muñiz, C., et al. (2021). First-and second-order phase transitions in RE_6Co_2Ga (RE= Ho, Dy or Gd) cryogenic magnetocaloric materials. Sci. China Mater. ***64***, 2846–2857.
175. Zhang, Z., Dong, X., Wang, Q., and Li, L. (2018). Investigation of the crystal structure, magnetic phase transition and magnetocaloric effect in $RE_5Ni_2In_4$ (RE= Dy, Ho and Er) compounds. Intermetallics ***100***, 136–141.
176. Zhang, Y., Xu, X., Yang, Y., et al. (2016). Study of the magnetic phase transitions and magnetocaloric effect in Dy_2Cu_2In compound. J. Alloys Compd. ***667***, 130–133.
177. Zhang, Y., Yang, Y., Xu, X., et al. (2016). Large reversible magnetocaloric effect in RE_2Cu_2In (RE= Er and Tm) and enhanced refrigerant capacity in its composite materials. J. Phys. D ***49***, 145002.
178. Li, L., Yi, Y., Su, K., et al. (2016). Magnetic properties and large magnetocaloric effect in Ho_2Cu_2In and Ho_2Au_2In compounds. J. Mater. Sci. ***51***, 5421–5426.
179. Bigun, I., Steinberg, S., Smetana, V., et al. (2017). Magnetocaloric behavior in ternary europium indides EuT_5In: probing the design capability of first-principles-based methods on the multifaceted magnetic materials. Chem. Mater. ***29***, 2599–2614.
180. Zhang, Z., Wang, P., Rong, H., and Li, L. (2019). Structural and cryogenic magnetic properties of RE_2Ni_2In (RE= Pr, Nd, Dy and Ho) compounds. Dalton Trans. ***48***, 17792–17799.
181. Zhang, Z., Stein, S., Li, L., and Poettgen, R. (2019). Magnetocaloric effect and critical behavior in ternary equiatomic magnesium compounds REPtMg (RE= Tb, Dy and Ho). Intermetallics ***109***, 24–29.
182. Li, L., Niehaus, O., Kersting, M., and Pöttgen, R. (2014). Reversible table-like magnetocaloric effect in Eu_4PdMg over a very large temperature span. Appl. Phys. Lett. ***104***, 092416.
183. Li, L., Niehaus, O., Kersting, M., and Pöttgen, R. (2015). Magnetic properties and magnetocaloric effect in the rare earth-rich phases RE_4PtMg (RE= Ho and Er). Intermetallics ***62***, 17–21.
184. Li, L., Niehaus, O., Kersting, M., and Pöttgen, R. (2015). Large reversible magnetocaloric effect around liquid hydrogen temperature in Er_4PdMg compound. IEEE T. Magn. ***51***, 1–4.
185. Li, L., Huo, D., Su, K., and Pöttgen, R. (2018). Magnetic properties and large magnetic entropy change in rare earth-rich cadmium compounds of RE_4CoCd (RE = Tm and Ho). Intermetallics ***93***, 343–346.
186. Guo, D., Wang, Y., Li, H., et al. (2019). Observation of large magnetocaloric effect in ternary Er-based Er_4CoCd compound. J. Magn. Magn. Mater. ***489***, 165462.
187. Yang, Y., Zhang, Y., Xu, X., et al. (2017). Magnetic and magnetocaloric properties of the ternary cadmium based intermetallic compounds of Gd_2Cu_2Cd and Er_2Cu_2Cd. J. Alloys Compd. ***692***, 665–669.
188. Zhang, Y., Yang, Y., Xu, X., et al. (2016). Excellent magnetocaloric properties in RE_2Cu_2Cd (RE= Dy and Tm) compounds and its composite materials. Sci. Rep. ***6***, 34192.
189. Yi, Y., Li, L., Su, K., et al. (2017). Large magnetocaloric effect in a wide temperature range induced by two successive magnetic phase transitions in Ho_2Cu_2Cd compound. Intermetallics ***80***, 22–25.
190. Gupta, S., and Suresh, K. (2013). Observation of giant magnetocaloric effect in HoCoSi. Mater. Lett. ***113***, 195–197.
191. Gupta, S.B., and Suresh, K. (2013). Giant low field magnetocaloric effect in soft ferromagnetic ErRuSi. Appl. Phys. Lett. ***102***, 022408.
192. Li, L., Hutchison, W.D., Huo, D., et al. (2012). Low-field giant reversible magnetocaloric effect in intermetallic compound $ErCr_2Si_2$. Scripta Mater. ***67***, 237–240.
193. Rawat, R., and Das, I. (2001). Magnetocaloric and magnetoresistance studies of $GdPd_2Si$. J. Phys. Condens. Matter ***13***, L57.
194. Rawat, R., and Das, I. (2006). Heat capacity and magnetocaloric studies of RPd_2Si (R= Gd, Tb and Dy). J. Phys. Condens. Matter ***18***, 1051.
195. Majumdar, S., Sampathkumaran, E., Paulose, P., et al. (2000). Anisotropic giant magnetoresistance, magnetocaloric effect, and magnetic anomalies in single crystalline Tb_2PdSi_3. Phys. Rev. B ***62***, 14207.
196. Sampathkumaran, E., Das, I., Rawat, R., and Majumdar, S. (2000). Magnetocaloric effect in Gd_2PdSi_3. Appl. Phys. Lett. ***77***, 418–420.
197. Pakhira, S., Mazumdar, C., Ranganathan, R., et al. (2016). Large magnetic cooling power involving frustrated antiferromagnetic spin-glass state in R_2NiSi_3 (R= Gd, Er). Phys. Rev. B ***94***, 104414.
198. Kumar, P., Singh, N.K., Suresh, K., and Nigam, A. (2008). Magnetocaloric and magnetotransport properties of R_2Ni_2Sn compounds (R= Ce, Nd, Sm, Gd, and Tb). Phys. Rev. B ***77***, 184411.
199. Li, L., Niehaus, O., Gerke, B., and Poettgen, R. (2014). Magnetism and magnetocaloric effect in EuAuZn. IEEE T. Magn. ***50***, 1–4.
200. Klenner, S., Zhang, Z., Poettgen, R., and Li, L. (2020). Magnetic and magnetocaloric properties of the equiatomic europium intermetallics EuAgZn, EuAgCd, EuPtZn and EuAuCd. Intermetallics ***120***, 106765.
201. Zhang, Y., and Wilde, G. (2016). Reversible table-like magnetocaloric effect in EuAuGe compound. J. Supercond. Nov. Magn. ***29***, 2159–2163.
202. Zeng, R., Dou, S., Wang, J., and Campbell, S.J. (2011). Large magnetocaloric effect in re-entrant ferromagnet $PrMn_{1.4}Fe_{0.6}Ge_2$. J. Alloys Compd. ***509***, L119-L123.
203. Kim, M., Sung, N., Son, Y., et al. (2011). Giant reversible anisotropic magnetocaloric effect in an antiferromagnetic $EuFe_2As_2$ single crystal. Appl. Phys. Lett. ***98***, 172509.
204. Castro, P.B.d., Terashima, K., Yamamoto, T.D., et al. (2020). Machine-learning-guided discovery of the gigantic magnetocaloric effect in HoB_2 near the hydrogen liquefaction temperature. NPG Asia Mater. ***12***, 35.
205. Li, J., Liu, Y., Lu, X., et al. (2021). Enhanced refrigeration capacity in $Ho_{1-x}Dy_xB_2$ compounds around liquid hydrogen temperature. J. Alloys Compd. ***864***, 158757.

206. Meng, H., Li, B., Han, Z., et al. (2012). Reversible magnetocaloric effect and refrigeration capacity enhanced by two successive magnetic transitions in DyB_2. Sci. China Technol. Sci. ***55***, 501–504.
207. Castro, P.B.d., Terashima, K., Yamamoto, T.D., et al. (2020). Effect of Dy substitution in the giant magnetocaloric properties of HoB_2. Sci. Technol. Adv. Mater. ***21***, 849–855.
208. Iwasaki, S., Yamamoto, T.D., de Castro, P.B., et al. (2022). Al substitution effect on magnetic properties of magnetocaloric material HoB_2. Solid State Commun. ***342***, 114616.
209. Han, Z., Li, D., Meng, H., et al. (2010). Magnetocaloric effect in terbium diboride. J. Alloys Compd. ***498***, 118–120.
210. Meng, L., Xu, C., Yuan, Y., et al. (2016). Magnetic properties and giant reversible magnetocaloric effect in $GdCoC_2$. Rsc Adv. ***6***, 74765–74768.
211. Li, D., Yamamura, T., Nimori, S., et al. (2013). Giant and isotropic low temperature magnetocaloric effect in magnetic semiconductor EuSe. Appl. Phys. Lett. ***102***, 152409.
212. Li, D., Yamamura, T., Nimori, S., et al. (2014). Large reversible magnetocaloric effect in ferromagnetic semiconductor EuS. Solid State Commun. ***193***, 6–10.
213. Hirayama, Y., Nakagawa, T., Kusunose, T., and Yamamoto, T.A. (2008). Magnetocaloric effect of rare earth nitrides. IEEE T. Magn. ***44***, 2997–3000.
214. Yamamoto, T.A., Nakagawa, T., Sako, K., et al. (2004). Magnetocaloric effect of rare earth mono-nitrides, TbN and HoN. J. Alloys Compd. ***376***, 17–22.
215. Nakagawa, T., Sako, K., Arakawa, T., and Yamamoto, T.A. (2004). Magnetocaloric effect of mononitride containing gadolinium and dysprosium $Gd_xDy_{1-x}N$. J. Alloys Compd. ***364***, 53–58.
216. Nakagawa, T., Sako, K., Arakawa, T., et al. (2006). Magnetocaloric effects of binary rare earth mononitrides, $Gd_xTb_{1-x}N$ and Tb_xJ. alloys and compounds. J. Alloys Compd. ***408***, 187–190.
217. Li, L., Nishimura, K., and Yamane, H. (2009). Giant reversible magnetocaloric effect in antiferromagnetic $GdCo_2B_2$ compound. Appl. Phys. Lett. ***94***, 102509.
218. Li, L., Nishimura, K., Usui, G., et al. (2012). Study of the magnetic properties and magnetocaloric effect in RCo_2B_2 (Rá= áTb, Dy and Ho) compounds. Intermetallics ***23***, 101–105.
219. Li, L., and Nishimura, K. (2009). Magnetic properties and large reversible magnetocaloric effect in $PrCo_2B_2$ compound. J. Appl. Phys. ***106***, 023903.
220. Li, L., and Nishimura, K. (2009). Magnetic properties and magnetocaloric effect in $NdCo_2B_2$ compound. J. Phys. D ***42***, 145003.
221. Li, L., Igawa, H., Nishimura, K., and Huo, D. (2011). Study of the magnetic transition and large magnetocaloric effect in $DyCo_3B_2$ compound. J. Appl. Phys. ***109***, 083901.
222. Li, L., Nishimura, K., Igawa, H., and Huo, D. (2011). Magnetic properties and magnetocaloric effect in $GdCo_3B_2$ compound. J. Alloys Compd. ***509***, 4198–4200.
223. Li, L., Huo, D., Igawa, H., and Nishimura, K. (2011). Large magnetocaloric effect in $TbCo_3B_2$ compound. J. Alloys Compd. ***509***, 1796–1799.
224. Zheng, X., Xu, J., Zhang, H., et al. (2018). Magnetic properties and magnetocaloric effect of $HoCo_3B_2$ compound. AIP Adv. ***8***, 056432.
225. Meng, L., Jia, Y., and Li, L. (2018). Study of the magnetic and magnetocaloric properties in RECoC (RE= Tb and Er) compounds. Intermetallics ***97***, 67–70.
226. Shi, C., Hu, W., Li, J., et al. (2022). Large magnetocaloric effect in antiferromagnetic ternary carbide $Dy_2Cr_2C_3$ around liquid hydrogen temperature. J. Magn. Magn. Mater. ***555***, 169339.
227. Zhang, Y., Li, S., Hu, L., et al. (2022). Excellent magnetocaloric performance in the carbide compounds $RE_2Cr_2C_3$ (RE= Er, Ho, and Dy) and their composites. Mater. Today Phys. ***27***, 100786.
228. Meng, L., Jia, Y., and Li, L. (2017). Large reversible magnetocaloric effect in the $RECoC_2$ (RE= Ho and Er) compounds. Intermetallics ***85***, 69–73.
229. Li, B., Hu, W., Liu, X., et al. (2008). Large reversible magnetocaloric effect in $TbCoC_2$ in low magnetic field. Appl. Phys. Lett. ***92***, 242508.
230. Zhang, Y., Guo, D., Wu, B., et al. (2020). Magnetic properties and magneto-caloric performances in $RECo_2B_2C$ (RE= Gd, Tb and Dy) compounds. J. Alloys Compd. ***817***, 152780.
231. Li, L., Nishimura, K., Kadonaga, M., et al. (2011). Giant magnetocaloric effect in antiferromagnetic borocarbide superconductor RNi_2B_2C (R= Dy, Ho, and Er) compounds. J. Appl. Phys. ***110***, 043912.
232. Zhang, Y., Geng, S., and Wilde, G. (2016). Magnetocaloric properties in $TbNi_2B_2C$ compound. J. Supercond. Nov. Magn. ***29***, 2681–2684.
233. Li, L., Kadonaga, M., Huo, D., et al. (2012). Low field giant magnetocaloric effect in RNiBC (R= Er and Gd) and enhanced refrigerant capacity in its composite materials. Appl. Phys. Lett. ***101***, 122401.
234. Li, L., Hirai, S., Nakamura, E., and Yuan, H. (2016). Influences of Eu_2O_3 characters and sulfurization conditions on the preparation of EuS and its large magnetocaloric effect. J. Alloys Compd. ***687***, 413–420.
235. Matsumoto, K., Li, L., Hirai, S., et al. (2016). Large magnetocaloric effect in sintered ferromagnetic EuS. Cryogenics ***79***, 45–48.
236. Delacotte, C., Pomelova, T.A., Stephant, T., et al. (2022). $NaGdS_2$: a promising sulfide for cryogenic magnetic cooling. Chem. Mater. ***34***, 1829–1837.
237. Yan, L., Shen, J., Li, Y., et al. (2007). Large magnetocaloric effect in spinel $CdCr_2S_4$. Appl. Phys. Lett. ***90***, 262502.
238. Dey, K., Indra, A., Karmakar, A., and Giri, S. (2020). Multicaloric effect in multiferroic sulpho spinel MCr_2S_4 (M= Fe & Co). J. Magn. Magn. Mater. ***498***, 166090.
239. Bouhbou, M., Moubah, R., Belayachi, W., et al. (2017). Magnetic and magnetocaloric properties in sulfospinel $Cd_{1-x}Zn_xCr_2S_4$ (x= 0, 0.3, 0.5) powders. Chem. Phys. Lett. ***688***, 84-88.
240. Tsurkan, V., Von Nidda, H.-A.K., Deisenhofer, J., et al. (2021). On the complexity of spinels: Magnetic, electronic, and polar ground states. Phys. Rep. ***926***, 1–86.
241. Nakagawa, T., Arakawa, T., Sako, K., et al. (2006). Magnetocaloric effects of ferromagnetic erbium mononitride. J. Alloys Compd. ***408***, 191–195.
242. Hirayama, Y., Tomioka, N., Nishio, S., et al. (2008). Magnetocaloric effect, specific heat and adiabatic temperature change of $Ho_xEr_{1-x}N$ (x= 0.25, 0.5, 0.75). J. Alloys Compd. ***462***, L12-L15.
243. Hirayama, Y., Nakagawa, T., Kusunose, T., and Yamamoto, T.A. (2007). Magnetocaloric effects of binary rare earth nitrides. MRS Online Proceedings Library (OPL) ***1040***, 1040–Q1009-1005.
244. Nishio, S., Nakagawa, T., Arakawa, T., et al. (2006). Specific heat and thermal conductivity of HoN and ErN at cryogenic temperatures. J. Appl. Phys. ***99***, 08K901.
245. Kim, D., Ahn, J., Sinha, B., et al. (2015). Novel route to prepare HoN nanoparticles for magnetic refrigerant in cryogenic temperature. Int. J. Hydrog. Energy ***40***, 11465–11469.
246. Shinde, K., Jang, S., Kim, J., et al. (2015). Magnetocaloric properties of TbN, DyN and HoN nanopowders prepared by the plasma arc discharge method. Dalton Trans. ***44***, 20386–20391.
247. Ahn, K., Pecharsky, A., Gschneidner, K., and Pecharsky, V. (2005). Preparation, heat capacity, magnetic properties, and the magnetocaloric effect of EuO. J. Appl. Phys. ***97***, 063901.
248. Yin, S., Sharma, V., McDannald, A., et al. (2016). Magnetic and magnetocaloric properties of iron substituted holmium chromite and dysprosium chromite. RSC Adv. ***6***, 9475–9483.
249. Oliveira, G., Pires, A., Machado, P., et al. (2019). Effect of chemical pressure on the magnetocaloric effect of perovskite-like $RCrO_3$ (R-Yb, Er, Sm and Y). J. Alloys Compd. ***797***, 269–276.
250. McDannald, A., Kuna, L., and Jain, M. (2013). Magnetic and magnetocaloric properties of bulk dysprosium chromite. J. Appl. Phys. ***114***, 113904.
251. Huang, R., Cao, S., Ren, W., et al. (2013). Large rotating field entropy change in $ErFeO_3$ single crystal with angular distribution contribution. Appl. Phys. Lett. ***103***, 162412.
252. Ke, Y.-J., Zhang, X.-Q., Ma, Y., and Cheng, Z.-H. (2016). Anisotropic magnetic entropy change in $RFeO_3$ single crystals (R= Tb, Tm, or Y). Sci. Rep. ***6***, 19775.
253. Das, M., Roy, S., and Mandal, P. (2017). Giant reversible magnetocaloric effect in a multiferroic $GdFeO_3$ single crystal. Phys. Rev. B ***96***, 174405.
254. Ke, Y.-J., Zhang, X.-Q., Wang, J.-F., and Cheng, Z.-H. (2018). Giant magnetic entropy change in gadolinium orthoferrite near liquid hydrogen temperature. J. Alloys Compd. ***739***, 897–900.
255. Midya, A., Khan, N., Bhoi, D., and Mandal, P. (2014). 3d-4f spin interaction and field-induced metamagnetism in $RCrO_4$ (R= Ho, Gd, Lu) compounds. J. Appl. Phys. ***115***, 17E114.
256. Palacios, E., Evangelisti, M., Sáez-Puche, R., et al. (2018). Magnetic structures and magnetocaloric effect in RVO_4 (R= Gd, Nd). Phys. Rev. B ***97***, 214401.
257. Balli, M., Mansouri, S., Dimitrov, D., et al. (2020). Strong conventional and rotating magnetocaloric effects in $TbVO_4$ crystals over a wide cryogenic temperature range. Phys. Rev. Mater. ***4***, 114411.
258. Moon, J., Kim, M., Oh, D., et al. (2018). Anisotropic magnetic properties and giant rotating magnetocaloric effect in double-perovskite Tb_2CoMnO_6. Phys. Rev. B ***98***, 174424.
259. Tkáč, V., Orendáčová, A., Čižmár, E., et al. (2015). Giant reversible rotating cryomagnetocaloric effect in $KEr(MoO_4)_2$ induced by a crystal-field anisotropy. Phys. Rev. B ***92***, 024406.
260. Phan, M.-H., and Yu, S.-C. (2007). Review of the magnetocaloric effect in manganite materials. J. Magn. Magn. Mater. ***308***, 325–340.
261. Chandra, S., Biswas, A., Phan, M.-H., and Srikanth, H. (2015). Impacts of nanostructuring and magnetic ordering of Nd^{3+} on the magnetic and magnetocaloric response in $NdMnO_3$. J. Magn. Magn. Mater. ***384***, 138–143.
262. Balli, M., Mansouri, S., Jandl, S., et al. (2016). Large rotating magnetocaloric effect in the orthorhombic $DyMnO_3$ single crystal. Solid State Commun. ***239***, 9–13.
263. Jin, J.-L., Zhang, X.-Q., Li, G.-K., et al. (2011). Giant anisotropy of magnetocaloric effect in $TbMnO_3$ single crystals. Physi. Rev. B ***83***, 184431.
264. Midya, A., Mandal, P., Das, S., et al. (2010). Magnetocaloric effect in $HoMnO_3$ crystal. Appl. Phys. Lett. ***96***, 142514.
265. Jin, J.-L., Zhang, X.-Q., Ge, H., and Cheng, Z.-H. (2012). Rotating field entropy change in hexagonal $TmMnO_3$ single crystal with anisotropic paramagnetic response. Phys. Rev. B ***85***, 214426.
266. Bohigas, X., Tejada, J., Del Barco, E., et al. (1998). Tunable magnetocaloric effect in ceramic perovskites. Appl. Phys. Lett. ***73***, 390–392.
267. Su, Y., Sui, Y., Cheng, J.-G., et al. (2013). Critical behavior of the ferromagnetic perovskites $RTiO_3$ (R= Dy, Ho, Er, Tm, Yb) by magnetocaloric measurements. Phys. Rev. B ***87***, 195102.
268. Omote, H., Watanabe, S., Matsumoto, K., et al. (2019). Magnetocaloric effect in single crystal $GdTiO_3$. Cryogenics ***101***, 58–62.

269. Mo, Z.-J., Shen, J., Li, L., et al. (2015). Observation of giant magnetocaloric effect in $EuTiO_3$. Mater. Lett. ***158***, 282–284.
270. Midya, A., Mandal, P., Rubi, K., et al. (2016). Large adiabatic temperature and magnetic entropy changes in $EuTiO_3$. Phys. Rev. B ***93***, 094422.
271. Balli, M., Roberge, B., Jandl, S., et al. (2015). Observation of large refrigerant capacity in the $HoVO_3$ vanadate single crystal. J. Appl. Phys. ***118***, 073903.
272. Dong, Q., Ma, Y., Ke, Y., et al. (2015). Ericsson-like giant magnetocaloric effect in $GdCrO_4$–$ErCrO_4$ composite oxides near liquid hydrogen temperature. Mater. Lett. ***161***, 669–673.
273. Palacios, E., Tomasi, C., Sáez-Puche, R., et al. (2016). Effect of Gd polarization on the large magnetocaloric effect of $GdCrO_4$ in a broad temperature range. Phys. Rev. B ***93***, 064420.
274. Midya, A., Khan, N., Bhoi, D., and Mandal, P. (2013). 3d-4f spin interaction induced giant magnetocaloric effect in zircon-type $DyCrO_4$ and $HoCrO_4$ compounds. Appl. Phys. Lett. ***103***, 092402.
275. Jiménez, E., Isasi, J., and Sáez-Puche, R. (2002). Field-induced magnetic properties in $RCrO_4$ oxides (R= Pr, Gd, Tb, Tm, and Yb). J. Solid State Chem. ***164***, 313–319.
276. Sáez-Puche, R., Jiménez, E., Isasi, J., et al. (2003). Structural and magnetic characterization of $RCrO_4$ oxides (R= Nd, Er and Tm). J. Solid State Chem. ***171***, 161–169.
277. Dey, K., Indra, A., Majumdar, S., and Giri, S. (2017). Cryogenic magnetocaloric effect in zircon-type RVO_4 (R= Gd, Ho, Er, and Yb). J. Mater. Chem. C ***5***, 1646–1650.
278. Midya, A., Khan, N., Bhoi, D., and Mandal, P. (2014). Giant magnetocaloric effect in antiferromagnetic $DyVO_4$ compound. Physica B Condens. Matter ***448***, 43–45.
279. Balli, M., Jandl, S., Fournier, P., and Gospodinov, M.M. (2014). Anisotropy-enhanced giant reversible rotating magnetocaloric effect in $HoMn_2O_5$ single crystals. Appl. Phys. Lett. ***104***, 232402.
280. Balli, M., Jandl, S., Fournier, P., and Dimitrov, D. (2016). Giant rotating magnetocaloric effect at low magnetic fields in multiferroic $TbMn_2O_5$ single crystals. Appl. Phys. Lett. ***108***, 102401.
281. Li, L., Wang, J., Su, K., et al. (2016). Magnetic properties and magnetocaloric effect in metamagnetic $RE_2Cu_2O_5$ (RE= Dy and Ho) cuprates. J. Alloys Compd. ***658***, 500–504.
282. Li, L., Su, K., and Huo, D. (2018). Large reversible normal and inverse magneto-caloric effects in the RE_2BaCuO_5 (RE= Dy and Er) compounds. J. Alloys Compd. ***735***, 773–776.
283. Zhang, Y., Li, H., Wang, J., et al. (2018). Structure and cryogenic magnetic properties in Ho_2BaCuO_5 cuprate. Ceram. Int. ***44***, 1991–1994.
284. Xu, P., Hu, L., Zhang, Z., et al. (2022). Electronic structure, magnetic properties and magnetocaloric performance in rare earths (RE) based RE_2BaZnO_5 (RE= Gd, Dy, Ho, and Er) compounds. Acta Mater. ***236***, 118114.
285. Tian, Y., Ouyang, J., Xiao, H., and Zhang, Y. (2021). Structural and magnetocaloric properties in the aeschynite type $GdCrWO_6$ and $ErCrWO_6$ oxides. Ceram. Int. ***47***, 29197–29204.
286. Ghara, S., Fauth, F., Suard, E., et al. (2018). Synthesis, structure, and physical properties of the polar magnet $DyCrWO_6$. Inorg. Chem. ***57***, 12827–12835.
287. Dhital, C., Pham, D., Lawal, T., et al. (2020). Crystal and magnetic structure of polar oxide $HoCrWO_6$. J. Magn. Magn. Mater. ***514***, 167219.
288. Panda, D.P., Yanda, P., Behera, S.S., and Sundaresan, A. (2022). Magnetic, magnetodielectric, and magnetocaloric properties of new polar oxides $RCrWO_6$ (R= Sm, Eu, Gd, and Tb). Solid State Commun. ***353***, 114843.
289. Jia, Y., Wang, Q., Wang, P., and Li, L. (2017). Structural, magnetic and magnetocaloric properties in R_2CoMnO_6 (R= Dy, Ho, and Er). Ceram. Int. ***43***, 15856–15861.
290. Sahoo, R., Das, S., and Nath, T. (2018). Role of Gd spin ordering on magnetocaloric effect and ferromagnetism in Sr substituted Gd_2CoMnO_6 double perovskite. J. Appl. Phys. ***124***, 103901.
291. Jia, Y., Wang, Q., Qi, Y., and Li, L. (2017). Multiple magnetic phase transitions and magnetocaloric effect in double perovskites R_2NiMnO_6 (R= Dy, Ho, and Er). J. Alloys Compd. ***726***, 1132–1137.
292. Dong, Z., Wang, Z., and Yin, S. (2020). Structural, magnetic and cryogenic magneto-caloric properties in RE_2FeCrO_6 (RE= Er and Tm) compounds. Ceram. Int. ***46***, 26632–26636.
293. Gardner, J.S., Gingras, M.J., and Greedan, J.E. (2010). Magnetic pyrochlore oxides. Rev. Mod. Phys. ***82***, 53.
294. Zhang, Y., Li, H., Guo, D., et al. (2018). Cryogenic magnetic properties in the pyrochlore RE_2TiMnO_7 (RE= Dy and Ho) compounds. Ceram. Int. ***44***, 15681–15685.
295. Cai, Y., Jiao, Y., Cui, Q., et al. (2017). Giant reversible magnetocaloric effect in the pyrochlore $Er_2Mn_2O_7$ due to a cooperative two-sublattice ferromagnetic order. Phys. Rev. Mater. ***1***, 064408.
296. Luo, X., Sun, Y., Hu, L., et al. (2009). Observation of the large magnetocaloric effect in an orbital–spin-coupled system MnV_2O_4. J. Phys. Condens. Matter ***21***, 436010.
297. Luo, X., Lu, W., Huang, Z., et al. (2012). Large reversible magnetocaloric effect in spinel MnV_2O_4 with minimal Al substitution. J. Magn. Magn. Mater. ***324***, 766–769.
298. Huang, Z., Luo, X., Hu, L., et al. (2014). Observation of the large magnetocaloric effect and suppression of orbital entropy change in Fe-doped MnV_2O_4. J. Appl. Phys. ***115***, 034903.
299. Shahi, P., Singh, H., Kumar, A., et al. (2014). Effect of Zn doping on the magneto-caloric effect and critical constants of Mott insulator MnV_2O_4. AIP Adv. ***4***, 097137.
300. Li, R., Li, G., and Greaves, C. (2018). Gaudefroyite: a mineral with excellent magnetocaloric effect suitable for liquefying hydrogen. J. Mater. Chem. A ***6***, 5260–5264.
301. Head, J., Manuel, P., Orlandi, F., et al. (2020). Structural, magnetic, magnetocaloric, and magnetostrictive properties of $Pb_{1-x}Sr_x MnBO_4$ (x= 0, 0.5, and 1.0). Chem. Mater. ***32***, 10184-10199.
302. Li, R. (2019). Enhancing the magnetocaloric effect of a paramagnet to above liquid hydrogen temperature. Energy Technol. ***7***, 1801070.
303. Tishin, A.M., and Spichkin, Y.I. (2016). The magnetocaloric effect and its applications. CRC Press. https://doi.org/10.1201/9781420033373.
304. McMichael, R.D., Ritter, J., and Shull, R. (1993). Enhanced magnetocaloric effect in $Gd_3Ga_{5-x}Fe_xO_{12}$. J. Appl. Phys. ***73***, 6946–6948.
305. Neupane, D., Hulsebosch, L., Ali, K.S., et al. (2022). Enhanced magnetocaloric effect in aluminum doped $Gd_3Fe_{5-x}Al_xO_{12}$ garnet: Structural, magnetic, and Mössbauer study. Materialia ***21***, 101301.
306. Sultana, J., Mohapatra, J., Liu, J.P., and Mishra, S.R. (2023). Structural, magnetic, and magnetocaloric properties of chromium doped $Gd_3Fe_{5-x}Cr_xO_{12}$ garnet compound. AIP Adv. ***13***, 025252.
307. Franco, V., Blázquez, J., Conde, C., and Conde, A. (2006). A Finemet-type alloy as a low-cost candidate for high-temperature magnetic refrigeration. Appl. Phys. Lett. ***88***, 042505.
308. Franco, V., Blázquez, J., and Conde, A. (2006). Field dependence of the magnetocaloric effect in materials with a second order phase transition: A master curve for the magnetic entropy change. Appl. Phys. Lett. ***89***, 222512.
309. Zhang, Y., Zuo, T.T., Tang, Z., et al. (2014). Microstructures and properties of high-entropy alloys. Prog. Mater. Sci. ***61***, 1–93.
310. Law, J.Y., and Franco, V. (2023). Review on magnetocaloric high-entropy alloys: Design and analysis methods. J. Mater. Res. ***38***, 37–51.
311. Law, J.Y., and Franco, V. (2021). Pushing the limits of magnetocaloric high-entropy alloys. APL Mater. ***9***, 080702.
312. Baker, M. (2021). Defining pathways for realizing the revolutionary potential of high entropy alloys: A TMS accelerator study. The Minerals, Metals & Materials Society.
313. Sheng, G., and Liu, C.T. (2011). Phase stability in high entropy alloys: Formation of solid-solution phase or amorphous phase. Prog. Nat. Sci. ***21***, 433–446.
314. Dong, Z., Wang, Z., and Yin, S. (2020). Magnetic properties and large cryogenic magneto-caloric effect of $Er_{0.2}Tm_{0.2}Ho_{0.2}Cu_{0.2}Co_{0.2}$ amorphous ribbon. Intermetallics ***124***, 106879.
315. Huo, J., Zhao, D., Bai, H., et al. (2013). Giant magnetocaloric effect in Tm-based bulk metallic glasses. J. Non. Cryst. Solids ***359***, 1–4.
316. Huo, J., Huo, L., Men, H., et al. (2015). The magnetocaloric effect of Gd-Tb-Dy-Al-M (M= Fe, Co and Ni) high-entropy bulk metallic glasses. Intermetallics ***58***, 31–35.
317. Yao, K., and Xu, Y. (2022). Magnetic properties, magnetic transition and large magneto-caloric effect in the $Ho_{0.2}Er_{0.2}Tm_{0.2}Ni_{0.2}Cu_{0.2}$ amorphous ribbon. Solid State Commun. ***345***, 114702.
318. Wang, Y., Guo, D., Wu, B., et al. (2020). Magnetocaloric effect and refrigeration performance in $RE_{60}Co_{20}Ni_{20}$ (RE= Ho and Er) amorphous ribbons. J. Magn. Magn. Mater. ***498***, 166179.
319. Zhang, Y., Zhu, J., Li, S., et al. (2022). Achievement of giant cryogenic refrigerant capacity in quinary rare-earths based high-entropy amorphous alloy. J. Mater. Sci. Technol. ***102***, 66–71.
320. Lucas, M., Belyea, D., Bauer, C., et al. (2013). Thermomagnetic analysis of $FeCoCr_xNi$ alloys: Magnetic entropy of high-entropy alloys. J. Appl. Phys. ***113***, 17A923.
321. Law, J.Y., Moreno-Ramírez, L.M., Díaz-García, Á., et al. (2021). MnFeNiGeSi high-entropy alloy with large magnetocaloric effect. J. Alloys Compd. ***855***, 157424.
322. Law, J.Y., Díaz-García, Á., Moreno-Ramírez, L.M., and Franco, V. (2021). Increased magnetocaloric response of FeMnNiGeSi high-entropy alloys. Acta Mater. ***212***, 116931.
323. Graedel, T.E., Barr, R., Chandler, C., et al. (2012). Methodology of metal criticality determination. Environ. Sci. Technol. ***46***, 1063–1070.
324. Wang, F., Harindintwali, J.D., Yuan, Z., et al. (2021). Technologies and perspectives for achieving carbon neutrality. The Innovation ***2***, 100180.
325. Law, J.Y., and Franco, V. (2021). Magnetocaloric Composite Materials. In Encyclopedia of Materials. Composites, pp. 461-472.
326. Li, L., Yuan, Y., Qi, Y., et al. (2018). Achievement of a table-like magnetocaloric effect in the dual-phase $ErZn_2$/ErZn composite. Mater. Res. Lett. ***6***, 67–71.
327. Chaturvedi, A., Stefanoski, S., Phan, M.-H., et al. (2011). Table-like magnetocaloric effect and enhanced refrigerant capacity in $Eu_8Ga_{16}Ge_{30}$-EuO composite materials. Appl. Phys. Lett. ***99***, 162513.

ACKNOWLEDGMENTS

Work funded by PID2019-105720RB-I00/AEI/10.13039/501100011033, Air Force Office of Scientific Research (FA8655-21-1-7044), the Clean Hydrogen Partnership and its members within the project HyLICAL (Grant No. 101101461), the European Innovation Council, funded by the European Union, via project CoCoMag (Grant no. 101099736), and the Research Council of Norway within project LIQUID-H. C. R.-M. acknowledges financial support by the Ramón y Cajal program of the Spanish Ministry of Science and

Innovation (Ref. RYC2021-031176-I). J.Y.L acknowledges EMERGIA 2021 fellowship from Junta de Andalucía (Ref. EMC21_00418).

AUTHOR CONTRIBUTIONS

C.R.-M., J.Y.L, J.R.-L. and L.M.M.-R. collected the data and revised the literature necessary for this work. C.R.-M and J.Y.L wrote the original manuscript. J.Y.L made the figures with some assistance from J.R.-M and L.M.M.-R. V.F. supervised all the tasks and revised the manuscript. All authors revised and contributed to the final edition of this article and approved the final submitted version.

DECLARATION OF INTERESTS

The authors declare no competing interests.

SUPPLEMENTAL INFORMATION

It can be found online at https://doi.org/10.59717/j.xinn-mater.2023.100045

LEAD CONTACT WEBSITE

The lead contact website is https://personal.us.es/vfranco